Quaternary Science Reviews 227 (2020) 106068

Contents lists available at ScienceDirect

Quaternary Science Reviews

journal homepage: www.elsevier.com/locate/quascirev

Seismic interpretation and structural restoration of the Heligoland glaciotectonic thrust-fault complex: Implications for multiple deformation during (pre-)Elsterian to Warthian ice advances into the southern North Sea Basin

Jutta Winsemann [a, *], Hannes Koopmann [a, b, 1], David C. Tanner [c], Rüdiger Lutz [b], Jörg Lang [a], Christian Brandes [a], Christoph Gaedicke [b]

[a] Institut für Geologie, Leibniz Universität Hannover, Callinstraße 30, 30167 Hannover, Germany
[b] Bundesanstalt für Geowissenschaften und Rohstoffe, Stilleweg 2, 30655 Hannover, Germany
[c] Leibniz Institut für Angewandte Geophysik, Stilleweg 2, 30655 Hannover, Germany

ARTICLE INFO

Article history:
Received 5 July 2019
Received in revised form
5 November 2019
Accepted 11 November 2019
Available online 18 November 2019

Keywords:
Glaciotectonics
Retrodeformation
North Sea
Pre-Elsterian ice-margin
Warthian ice-margin
Tunnel valley

ABSTRACT

Despite a long history of research, the locations of former ice-margins in the North Sea Basin are still uncertain. In this study, we present new palaeogeographic reconstructions of (pre-) Elsterian and Warthian ice-margins in the southeastern North Sea Basin, which were previously unknown. The reconstructions are based on the integration of palaeo-ice flow data derived from glaciotectonic thrusts, tunnel valleys and mega-scale glacial lineations. We focus on a huge glaciotectonic thrust complex located about 10 km north of Heligoland and 50 km west of the North Frisian coast of Schleswig-Holstein (Northern Germany). Multi-channel high-resolution 2D seismic reflection data show a thrust-fault complex in the upper 300 ms TWT (ca. 240 m) of seismic data. This thrust-fault complex consists of mainly Neogene delta sediments, covers an area of 350 km^2, and forms part of a large belt of glaciotectonic complexes that stretches from offshore Denmark via northern Germany to Poland. The deformation front of the Heligoland glaciotectonic complex trends approximately NNE-SSW. The total length of the glaciotectonic thrust complex is approximately 15 km. The thrust faults share a common detachment surface, located at a depth of 250–300 ms (TWT) (200–240 m) below sea level. The detachment surface most probably formed at a pronounced rheological boundary between Upper Miocene fine-grained pro-delta deposits and coarser-grained delta-front deposits, although we cannot rule out that deep permafrost in the glacier foreland played a role for the location of this detachment surface. Restored cross-sections reveal the shortening of the complex along the detachment to have been on average 23% (ranging from ca. 16%–50%). The determined ice movement direction from east-southeast to southeast suggests deformation by an ice advance from the Baltic region. The chronospatial relationship of the thrust-fault complex and adjacent northwest-southeast to northeast-southwest trending Elsterian tunnel valleys implies a pre-Elsterian (MIS 16?) age of the glaciotectonic complex. However, the age of these Elsterian tunnel valleys is poorly constrained and the glaciotectonic complex of Heligoland may also have been formed during an early Elsterian ice advance into the southeastern North Sea Basin. The glaciotectonic complex underwent further shortening and the Elsterian tunnel-valley fills that were incised into the glaciotectonic complex were partly deformed during the Saalian Drenthe and Warthe (1) ice advances.

1. Introduction

The location and behaviour of pre-Weichselian ice sheets in the North Sea Basin is still uncertain (Ehlers et al., 2011; Böse et al., 2012; Lee et al., 2012; Stewart et al., 2013; Cohen et al., 2014;

* Corresponding author.
E-mail address: winsemann@geowi.uni-hannover.de (J. Winsemann).
[1] now at: COWI A/S, Havneparken 1, 7100 Vejle, Denmark.

https://doi.org/10.1016/j.quascirev.2019.106068

Phillips et al., 2017), but can be analysed by the orientation of subglacial tunnel valleys, mega-scale glacial lineations, glaciotectonic complexes, and their chronospatial relationships. The traditional view of the Pleistocene glaciation history of the central and southern North Sea Basin is that major grounded ice-sheets did not develop before Marine Isotope Stage 12 (Toucanne et al., 2009; Ehlers et al., 2011; Stewart and Lonergan, 2011; Stewart et al., 2013; Cohen et al., 2014; Stewart, 2016). However, there is growing evidence for an Early Pleistocene or early Middle Pleistocene onset of glaciation (e.g., Moreau et al., 2012; Buckley, 2017; Bendixen et al., 2018; Ottesen et al., 2018; Rea et al., 2018).

During the Pleistocene glaciations, large glaciotectonic complexes formed in northern central Europe due to the advance of the ice sheets. These glaciotectonic complexes partly have had a complex, multiphase evolution and have been the focus of attention for more than a century; especially from the mid-1980s onwards (e.g., Aber, 1982; Van der Wateren, 1985; Feeser, 1988; Ingólfsson, 1988; Van der Wateren, 1995; Huuse and Lykke-Andersen, 2000b; Andersen et al., 2005; Burke et al., 2009; Pedersen, 2005; Aber and Ber, 2007; Thomas and Chiverrell, 2007; Phillips et al., 2002, 2008; Lee et al., 2013; Szuman et al., 2013; Lee et al., 2017; Kowalski et al., 2019). In recent years, glaciotectonic complexes have been increasingly studied with high-resolution reflection seismic data, often in offshore areas (Pedersen, 2014; Cotterill et al., 2017; Dove et al., 2017; Pedersen and Boldreel, 2017; Vaughan-Hirsch and Phillips, 2017; Bendixen et al., 2018; Phillips et al., 2018; Roberts et al., 2018). This allows the analysis of the style of deformation at large spatial scales, overcoming the common spatial limitations of onshore outcrops.

Glaciotectonic deformation is controlled by the ice-bed coupling, which in turn depends on the thermo-mechanical properties of the ice and substrate. The most important factors are i) the thermal properties of the substrate; ii) the permeability and porosity of the substrate; iii) the porewater availability and iv) the presence of a potential detachment layer (e.g., Rutten, 1960; Van der Wateren, 1985; Astakhov et al., 1996; Boulton, 1996; Etzelmüller et al., 1996; Boulton et al., 1999; Huuse and Lykke-Andersen, 2000b; Piotrowski et al., 2004; Lee and Phillips, 2008; Waller et al., 2009, 2012; Szuman et al., 2013).

Glaciotectonic complexes do not form at every ice margin and may require specific glaciological conditions and/or the occurrence of conditions favourable for deformation in the glacier foreland (e.g., Bennett, 2001). Important aspects are the potential association with fast ice-flow (e.g., Croot, 1988; Ó Cofaigh et al., 2010; Vaughan-Hirsch and Phillips, 2017) and ice-marginal permafrost. Ice-marginal permafrost may extend the zone of porewater overpressure much further beyond the glacier than in non-permafrost settings. In addition, the presence of interstitial ice within the pore space increases cohesion and the shear strength of the frozen sediment. Stress can be transmitted over a considerable distance by the relatively stiff frozen sediments, and thus probably fostering the formation of large and broad glaciotectonic complexes (e.g., Rutten, 1960; Kälin, 1971; Etzelmüller et al., 1996; Boulton et al., 1999; Hiemstra et al., 2007; Burke et al., 2009; Waller et al., 2009, 2012). However, glaciotectonic complexes do not, in general, provide evidence for the existence of ice-marginal permafrost (e.g., Tsui et al., 1989).

Therefore, in addition to porewater, rheology of the underlying sediment plays an important role in the formation of glaciotectonic thrust-fault complexes, independent of whether they are on- or offshore. Glaciotectonic complexes are comparable to thin-skinned fold-and-thrust belts, in terms of geometry and formation (Aber, 1982; Croot, 1987; Brandes and Le Heron, 2010; Cotterill et al., 2017; Vaughan-Hirsch and Phillips, 2017). Glacial pushing (bulldozing) is a major process in glaciotectonic complex formation (Bennett, 2001). Pedersen (1987) identified the process of gravity spreading to be responsible for glaciotectonic deformation. Research has also focused on the role of bedrock topography to explain the complex internal geometry of some complexes (Dobrowolski and Terpilowski, 2006), the interaction of glaciotectonic deformation and underlying pre-existing fault systems (Włodarski, 2014) or salt structures (Lang et al., 2014).

Analysing such glaciotectonic complexes is important because they allow the determination of the maximum extent of glaciers and ice sheets, whilst also providing information on ice-marginal dynamics and the interaction of an ice-sheet with its foreland (Bennett, 2001; Pedersen, 2005; Madsen and Piotrowski, 2012; Bendixen et al., 2018; Gehrmann and Harding, 2018; Roberts et al., 2018; Mellett et al., 2019). Traditionally, the mapped extent of tills, their clast provenance and clast fabric have been used to reconstruct ice limits and the direction of ice advances (e.g., compilations in Skupin and Zandstra, 2010; Ehlers et al., 2011; Houmark-Nielsen, 2011; Laban and van der Meer, 2011; Lang et al., 2018; Stephan, 2019). However, not all ice advances may produce till, and the thickness and spatial distribution of till strongly depends on ice-flow velocity and substrate conditions (e.g., Boulton, 1996; Jørgensen and Piotrowski, 2003; Kjær et al., 2003; Passchier et al., 2010). Thin till covers and/or terminal moraines may be rapidly eroded by subsequent (post-)glacial processes (e.g., Gibbons et al., 1984; Boulton, 1996; Rasmussen et al., 2010; Moreau et al., 2012; Stephan, 2014). Therefore, seismic analysis of large glaciotectonic complexes provides the best evidence for ice fronts, and the structural analysis and restoration of these complexes allow the reconstruction regional ice-flow patterns, ice-sheet behaviour and advance-retreat cycles (Pedersen, 1996, 2005; Lee et al., 2013; Gehrmann and Harding, 2018; Phillips et al., 2018). In addition, the glaciotectonic complexes may provide data on the substrate conditions and porewater availability in the glacier foreland (Boulton, 1996, 1999; Waller et al., 2009, 2012; Lee et al., 2013; Vaughan-Hirsch and Phillips, 2017). Smaller push moraines can help to understand the nature of rapid ice-marginal fluctuations (Bennett et al., 2004) and the pattern of active retreat (e.g., Lee et al., 2013; Cotterill et al., 2017; Phillips et al., 2018).

This paper focuses on a huge glaciotectonic thrust complex, located about 10 km north of Heligoland and 50 km west of the North Frisian coast of Schleswig-Holstein (Fig. 1A–C). It was previously described by Borth-Hoffmann (1980) and Figge (1983), who analysed single-channel seismic data. Both authors observed the occurrence of eastward-to southeastward-dipping glaciotectonic thrusts to the north of Heligoland. However, the deformation history and palaeogeographic significance of the Heligoland glaciotectonic complex was not discussed in detail.

Selected profiles of about 6500 km, multi-channel, high-resolution, 2D seismic data were used in this work. It was acquired by the Federal Institute for Geosciences and Natural Resources (Bundesanstalt für Geowissenschaften und Rohstoffe, BGR) during three research cruises (BGR03-AUR, BGR04-AUR and HE242 Leg 1). These data provide detailed insight into the structure and geometry of this buried fault complex and offer implications for the maximum advances of (pre-)Elsterian to early Warthian (Warthe 1) ice sheets in this area. We present these unpublished seismic lines around the island of Heligoland and use the interpretations to derive structurally-balanced cross-sections. Based on the interpretation of the geophysical dataset, we calculate the amount of shortening, derive the force directions acting on the sediment during the Middle Pleistocene (pre-)Elsterian to Warthian ice advances, discuss the controlling factors for the location of the detachment horizon, and develop a schematic model for the deformation history of the glaciotectonic complex. Based on the integration of

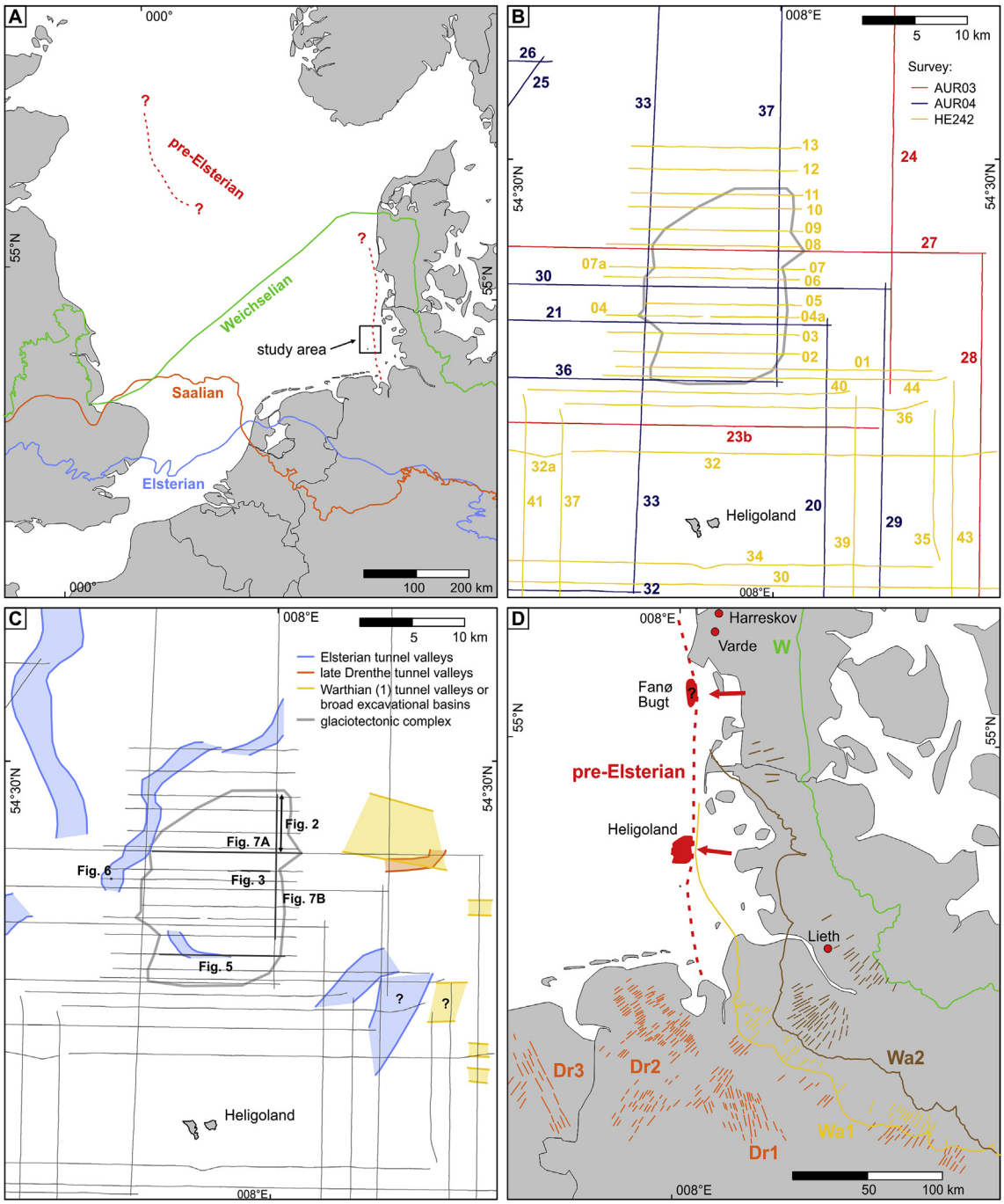

Fig. 1. Location of the study area. A) Overview map, showing the maximum extent of the Middle Pleistocene pre-Elsterian (Don ?), Elsterian, Saalian (Drenthe) and Late Pleistocene Weichselian ice sheets in northern central Europe. The ice margins are modified after Ehlers et al. (2011); Roskosch et al. (2015); Hughes et al. (2016); Bendixen et al. (2018); Lang et al. (2018). B) Map of the seismic lines around Heligoland used in this study. C) Close-up view of the study area, showing three different generations of tunnel valleys (modified after Lutz et al., 2009) and the outline of the mapped glaciotectonic complex of Heligoland. D) Infered margin of a pre-Elsterian (Don?) ice advance (in red) into the southern North Sea Basin. Red dots indicate the occurrence of pre-Elsterian till and meltwater deposits (compiled from Vinx et al., 1997; Houmark-Nielsen, 2011; Høyer et al., 2013). Red arrows indicate the reconstructed ice-flow direction (this study; Huuse and Lykke-Andersen, 2000b). Dr1-Dr3 refer to mega-scale glacial lineation of the older Saalian Drenthe ice advances (modified after Lang et al., 2018). The Warthe 1 ice advance into the southern North Sea Basin is inferred from the mapped E-W trending tunnel valleys and mapped mega-scale glacial lineations on land. The Warthe 2 ice margin (Wa2) and Weichselian (W) ice margin are modified after Ehlers et al. (2011) and Hughes et al. (2016). (For interpretation of the references to colour in this figure legend, the reader is referred to the Web version of this article.)

palaeo-ice flow data derived from the glaciotectonic-thrust complex, mapped tunnel valleys and mega-scale glacial lineations, we present new palaeogeographic reconstructions of previously unknown (pre-) Elsterian and Warthian ice-margins in the south-eastern North Sea Basin.

2. Geological setting

During the Cenozoic, the North Sea area was an epicontinental basin, confined by vast landmasses (Ziegler, 1990; Knox et al., 2010; Gibbard and Lewin, 2016; Cohen et al., 2017; Ottesen et al., 2018). The sedimentation in the southern North Sea basin was dominated

by a large delta system, referred to as the Eridanos Delta. Its drainage area covered most of the Fennoscandian and Baltic shields from Miocene to Pleistocene times (Cameron et al., 1993; Overeem et al., 2001; Knox et al., 2010; Thöle et al., 2014). Delta progradation occurred mainly from the Northeast and East and subsequently from the Southeast, leading to the deposition of increasingly younger delta deposits in the German and Dutch sectors of the North Sea (Thöle et al., 2014). The deposition of the Eridanos Delta started in the Late Miocene and delta deposits are separated from the underlying Middle Miocene to Paleocene deposits by a prominent unconformity, the so-called Mid-Miocene Unconformity (MMU), which represents an interval of condensed sedimentation in the southern North Sea Basin, related to a major transgression (Huuse and Clausen, 2001; Thöle et al., 2014). This unconformity dips towards the Northwest (Central North Sea Graben), from less than 200 ms (TWT) close to the coast to more than 1400 ms (TWT) in the Entenschnabel area. The whole surface is pierced and uplifted by several salt structures (Thöle et al., 2014).

After this transgression, the sediment input strongly increased and delta progradation started. The increase in sediment supply may be related to uplift of the basin margins and/or climate detoriation (Nielsen et al., 2009; Rasmussen, 2009; Knox et al., 2010; Thöle et al., 2014; Arfai et al., 2014, 2018; Deckers and Louwye, 2019). Frequent sea-level changes during the Neogene influenced the delta architecture and led to the development of several unconformities (Thöle et al., 2014).

The beginning of the Pleistocene was marked by a regression of sea level and subsequent deposition of fluvio-deltaic sediments on the shelf, mainly sourced by rivers entering from the east and southeast into the North Sea Basin (Overeem et al., 2001; Kuhlmann et al., 2004; Streif, 2004; Gibbard and Lewin, 2009, 2016; Thöle et al., 2014; Winsemann et al., 2015; Cohen et al., 2017; Benvenuti et al., 2018; Ottesen et al., 2018; Deckers and Louwye, 2019). Delta sedimentation probably persisted until the Middle Pleistocene in the study area (Thöle et al., 2014). The growing Middle Pleistocene Fennoscandian ice sheets strongly impacted the large Eridanos River system by blocking drainage pathways and forced many tributary rivers into new courses (e.g., Overeem et al., 2001; Cohen et al., 2014; Thöle et al., 2014; Winsemann et al., 2015; Cohen et al., 2017; Panin et al., in review). By the Middle Pleistocene, the Eridanos River system had apparently lost the connection to the Fennoscandian and Baltic headwaters (Gibbard and Lewin, 2016). Increased glacial erosion of the Baltic Sea area since the Middle Pleistocene Saalian glaciation (e.g., Meyer, 1991) eventually led to the change of river drainage pathways and the reorganisation of river systems in central and northern Europe.

The first ice advance may have reached the study area during the Menapian (MIS 34). During this glaciation, the so-called Fedje Till (central North Sea Basin) and the Hattem Beds (Netherlands and northwestern Germany) were deposited (Ehlers et al., 2011; Graham et al., 2011; Laban and van der Meer, 2011; Lee et al., 2012, and references therein). The Harreskov Till in Denmark and the assumed pre-Elsterian till near Lieth in northern Germany (Fig. 1D) may correspond to this glaciation or a younger glaciation during the Cromerian Complex (e.g., Vinx et al., 1997; Houmark-Nielsen, 2011; Høyer et al., 2013). These pre-Elsterian tills are characterised by erratic clasts from western Scandinavian source areas, pointing to ice-advances from the North to Northeast (e.g., Kronborg, 1986; Meyer, 1991; Vinx et al., 1997; Stephan, 2014).

During the subsequent Middle Pleistocene glacial periods, the study area was repeatedly transgressed by the Fennoscandian ice sheets. The age of the Elsterian glaciations in the Netherlands, northern Germany and Denmark is still under discussion, and correlation problems still persist (e.g., Litt et al., 2007; Ehlers et al., 2011; Houmark-Nielsen, 2011; Böse et al., 2012; Lee et al., 2012; Roskosch et al., 2015; Lauer and Weiss, 2018).

Up to three Elsterian ice-advances have been recorded. These ice advances occurred from the North, then Northeast and finally from the East, as indicated by the clast composition of tills and the orientation of subglacial tunnel valleys (Huuse and Lykke-Andersen, 2000a; Jørgensen and Sandersen, 2006; Lutz et al., 2009; Stackebrandt, 2009; Houmark-Nielsen, 2011; Ehlers et al., 2011; Hepp et al., 2012; Lang et al., 2012; Stephan, 2014, 2019; Stewart, 2016; Sandsersen and Jørgensen, 2017; Coughlan et al., 2018). These three ice advances are now commonly correlated with MIS 12, but also MIS 10 ages have been discussed (Litt et al., 2007; Toucanne et al., 2009; Ehlers et al., 2011; Houmark-Nielsen, 2011; Böse et al., 2012; Lee et al., 2012; Lang et al., 2012; Roskosch et al., 2015; Lauer and Weiss, 2018). From the subsequent Saalian glaciations, three major ice advances, with several subphases are known; they are referred to as the Drenthe and Warthe ice advances. The Drenthe stage is also referred to as the older Saalian Glaciation, the first Warthe advance (Warthe 1) as middle Saalian Glaciation and the second Warthe ice advance (Warthe 2) as late Saalian Glaciation (Fig. 1A, D). All these ice advances are correlated with MIS 6 and were caused by ice moving from the North, Northeast and East (Busschers et al., 2008; Ehlers et al., 2011; Houmark-Nielsen, 2011; Böse et al., 2012; Roskosch et al., 2015; Lang et al., 2018; Lauer and Weiss, 2018; Stephan, 2019), but also an extensive earlier Saalian ice advance during MIS 8 has been discussed (e.g., Beets et al., 2005; Lee et al., 2012; Roskosch et al., 2015).

Key elements for the offshore Quaternary stratigraphy are tunnel-valley fills. They are found across the entire North Sea Basin and are easily identified in seismic sections. Their directions, shapes and cross-cutting relationships allow the reconstruction of different ice-advances and the establishment of a relative stratigraphic framework. In the central and southern North Sea Basin, up to seven generations of tunnel valleys have been incised into older Pleistocene and Neogene deposits (e.g., Sejrup et al., 2005; Lonergan et al., 2006; Kristensen et al., 2007; Lutz et al., 2009; Stewart and Lonergan, 2011; Stewart et al., 2013; Stewart, 2016; Sandsersen and Jørgensen, 2017). These different tunnel valley generations may record an equivalent number of separate advance and retreat cycles of ice sheets (Stewart and Lonergan, 2011; Stewart et al., 2013; Stewart, 2016) or simply multiple ice advances within a single glaciation (Kristensen et al., 2007). In general, the age of the tunnel valleys in the North Sea Basin is poorly constrained and age estimates are based on correlation with onshore data and dated tunnel valleys from the Dutch and Danish North Sea sectors. In the southern North Sea and onshore Netherlands, Germany, and eastern England, the oldest tunnel valleys are inferred to be mainly Elsterian in age (MIS 12), because overlying or interbedded interglacial deposits yield Holsteinian ages and tunnel valleys partly truncate deposits assigned to the Cromerian Complex, giving a maximum age for the study area (e.g., Kuster and Meyer, 1979; Stackebrandt, 2009; Lee et al., 2012; Hepp et al., 2012; Lang et al., 2012; Janszen et al., 2013; Cohen et al., 2014; Steinmetz et al., 2015). However, absolute ages are scarce and the oldest tunnel-valley fills may be partly older than MIS 12 (e.g., Buckley, 2017; Høyer et al., 2013), or may have formed during MIS 10, as is indicated by absolute ages of tunnel-valley fills onshore in northern Germany (Lang et al., 2012, 2015; Roskosch et al., 2015) and Elsterian deposits in the northeastern Netherlands (Lee et al., 2012; F.S. Busschers, pers. comm.). These tunnel valleys were later often re-used during subsequent younger glaciations or rivers, as indicated by a complex valley-fill archtitecture with multiple cut- and fill structures (e.g. Huuse and Lykke-Andersen, 2000a;

Larsen and Andersen, 2005; Stackebrandt, 2009; Lang et al., 2012; Janszen et al., 2013; Moreau and Huuse, 2014; Steinmetz et al., 2015; Sandsersen and Jørgensen, 2017; Benvenuti et al., 2018; Prins and Andresen, 2019). The Weichselian ice-sheet did not reach the study area, implying that all tunnel valleys must be older than MIS 4 (Larsen et al., 2009; Houmark-Nielsen, 2011; Böse et al., 2012; Hughes et al., 2016).

3. Data base and methods

3.1. Seismic dataset

In this study, we use high-resolution, multichannel seismic profiles from three scientific cruises in the North Sea that were conducted by BGR between 2003 and 2005 (Fig. 1B). The BGR03-AUR cruise in 2003 (Kudraß, 2003) and the BGR04-AUR cruise in 2004 (Neben, 2004) acquired seismic profiles of about 2500 km and 2600 km length, respectively. An additional 1400 km of high-resolution multichannel seismic data were acquired in 2005 during cruise HE242 Leg 1 (Neben, 2006). All three cruises aimed mainly at shallow structures down to 1 s (TWT). The onboard scientific party processed the data. Water depths during cruises were in the range of 7–50 m on BGR03-AUR, and about 15 m on HE242.

The equipment used on all three cruises for the generation and acquisition of acoustic waves consisted of a generator-injector-gun (GI-Gun, type 645-100) and a 300 m streamer. Both (generator and injector) chambers of the gun operated with a volume reducer and therefore with effective volumes of 25 cubic inches each, albeit in a single casing. The total volume of the system was 50 cubic inches (0.82 l). The GI-Gun was fired at a pressure of 14–15 MPa every 12.5 m. Both source and receivers had a nominal towing depth of 2–3 m below surface. The 300 m streamer consisted of four active seismic sections of 75 m length, each equipped with six channels, resulting in a channel spacing of 12.5 m on the active sections and 24 channels. The usable bandwidth at a depth of 2 m was 300 Hz, with frequencies between 25 and 325 Hz. Data were recorded at a sampling rate of 0.5 ms (2 kHz), thus the Nyquist frequency was 1 kHz, meaning all data within the usable bandwidth were sampled. Penetration depth was usually between 1 and 2 s (TWT), which is more than sufficient to image the upper 300–500 ms (TWT) of interest in this study.

Only selected profiles were used in this study, which reduced the dataset to 2000 km of seismic profiles around, but mostly north of Heligoland. Not all of these profiles are directly relevant to the glaciotectonic structure, since the complex is smaller than the area covered by the seismic profiles (Fig. 1B and C). Depth conversion was carried out by applying an average velocity of 1600 m/s to the studied interval. This value is a simplification, but it matches very well with our previous studies based on stacking velocities and calculated average velocities (Lutz et al., 2009).

3.2. Echosounder data

A parametric Innomar SES-2000 standard echosounder was deployed during cruise HE242 to collect shallow subsurface information. The echosounder data were recorded parallel to the high-resolution seismic data used for this study. The penetration depth was in the range of 3–10 m, depending on the grain size. Data gaps occurred only during very rough weather conditions, which hampered sound transmission. The system operated with a primary frequency of 100 kHz and secondary frequencies of 4, 5, 6, 8, 10, and 12 kHz. Because of the high system bandwidth of a parametric system, short signals can be transmitted without ringing. This makes parametric systems useful in particular in shallow water areas (Wunderlich and Müller, 2003).

3.3. Kinematic restoration

Five seismic sections (AUR03_27, AUR04_30, AUR04_27, HE242_05, HE242_09), which cover most of the deformed part of the glaciotectonic complex, were selected for restoration (see Fig. 1B and C for location of seismic sections). The software 2DMove (Petex Ltd) was used for structural restoration. Kinematic restoration was carried out using the principle of minimum displacement, i.e., beds were constructed so they were cutoff by the faults directly after they could not be seen in the seismic anymore. In addition, horizons were extended to make contact with the faults. Furthermore, minor changes in fault geometry had to be made to balance the cross-sections. The analysed glaciotectonic complex is characterised by in-sequence thrusting. Kinematic restoration therefore began at the foreland pin and progressed backwards through the thrust-fault complex. The fault-parallel flow algorithm was used for kinematically retrodeformation (cf. Ziesch et al., 2014).

3.4. Reconstructions of ice advances

The directions of ice-advances were derived from the orientation of mega-scale glacial lineations, tunnel valleys and glaciotectonic thrusts. Mega-scale glacial lineations and tunnel valleys are considered to form parallel to the ice-flow lines (e.g., Clark, 1993; Boulton et al., 2001; Kehew et al., 2012). The deformation fronts of proglacial glaciotectonic complexes trend parallel to the ice-margin and the dip direction of thrust faults is up-ice (e.g., Aber, 1982; Van der Wateren, 1985; Feeser, 1988; Bennett, 2001; Pedersen, 2005).

An extensive database of regional studies provides data on palaeo-ice flow directions and till provenance. Major results on till provenance, till-clast fabric, glacial striations, mega-scale glacial lineations and glacitectonic deformation structures of the onshore study area are compiled in Ehlers and Stephan (1983), Ehlers et al. (2011), Houmark-Nielsen (2011), Lang et al. (2018) and Stephan (2019). Regional palaeo-ice flow directions derived from onshore and offshore tunnel valleys are summarized in Lutz et al. (2009), Stackebrandt (2009), and Sandsersen and Jørgensen (2017).

For this study, additional mega-scale glacial lineations were mapped from digital elevation models (grid ~30 m), vertical accuracy ~3 m (EU-DEM) of the northeastern onshore part of the study area (Fig. 1D) and tunnel valleys from seismic sections of the eastern offshore study area (Fig. 1C), which was not entirely covered by Lutz et al. (2009).

For the Heligoland seismic data, the internal architecture and dip direction of glaciotectonic thrusts were used to reconstruct the deformation history and related ice-push direction. As the acquired 2 D seismic lines trend oblique to the true dip direction of the Heligoland glaciotectonic complex, the sections only image the apparent dip and plunge directions of thrust faults. These apparent dip and plunge values were used to calculate true dip and plunge values, following the method of Meissner and Stegena (1977). For calculation, eight composite seismic 2D sections were depth converted and 28 dip values of first generation thrust faults were measured. The calculated dip direction values were subsequently plotted in a rose diagram.

4. Results

4.1. Interpretation of seismic data

4.1.1. Mapped seismostratigraphic units

Within the glaciotectonic thrust-fault complex, four seismic units were mapped, which are separated by distinct seismic

reflectors that represent major depositional or erosional boundaries (Figs. 2 and 3). The lithology and age of these seismic units is not exactly known, because no borehole data are available for the Heligoland glaciotectonic complex. Based on correlation with borehole data and dated undeformed seismostratigraphic units located approximately 80 km further southeast onshore (Gramann, 1989; Kuster, 2005; Steinmetz et al., 2015) and 80 km further northwest offshore (Köthe, 2012; Thöle et al., 2014), we infer that the deformed succession mainly comprises Upper Miocene delta sediments. The prominent Mid-Miocene unconformity (MMU) is located 100–200 ms (TWT) (ca. 80–160 m) below the basal detachment of the glaciotectonic complex, which lies at a depth of 250–300 ms (TWT) (ca. 200–240 m) below sea level (Fig. 3). The basal detachment surface may therefore have been developed at the boundary between Upper Miocene fine-grained shelf or pro-delta deposits (green, seismic unit 1) and coarser-grained Upper Miocene delta-front deposits (violet, seismic unit 2). Seismic unit 3 (orange) may represent the uppermost Tortonian delta-front/delta-plain deposits, overlain by Messinian delta-front/delta-plain deposits (yellow, seismic unit 4).

4.1.2. Glaciotectonic deformation

Within the glaciotectonic thrust-fault complex, 327 thrust faults on 21 seismic sections were mapped (deformation phase D1). Correlation of the mapped faults from section to section was not possible as the line spacing of the seismic profiles is too large. The area in which the faults were mapped covers ca. 350 km^2 (Fig. 1B and C). Although the thrust faults show a great variety with respect to their dip angles and offsets, some features are remarkably similar. For the most part of the complex, the observed faults can be considered listric (concave up) thrust faults that join a common detachment at 250–300 ms TWT (ca. 200–240 m depth).

Geometry of the faults varies over a broad range; very steep faults that show only slight listric geometry can be mapped right next to fault-bend folds with a typical flat-ramp-flat geometry (Figs. 2 and 3). Some of these shallow-dipping, fault-bend folds are responsible for transport of the sediment package by up to 1500 m in the transport direction (Figs. 2 and 3).

Only three of the N–S striking sections cover the whole glaciotectonically deformed area. Derived true fault dip directions from seismic profile intersections are mainly southeast- or east dip directions (Fig. 4). As correlation was only rarely possible, the true number of thrust-sheets is significantly smaller than suggested by the number of 327 mapped faults. From these plots, the derived main area of deformation is located north of seismic section HE242_03 and south of seismic section HE242_10 (Fig. 1B and C).

Of the mapped faults, 19% of the faults are back-thrusts. Some back-thrusts are in positions relative to other faults such that they form triangle zones, which are usually located in other settings, such as in the foreland or distal end of a fold-and-thrust belt

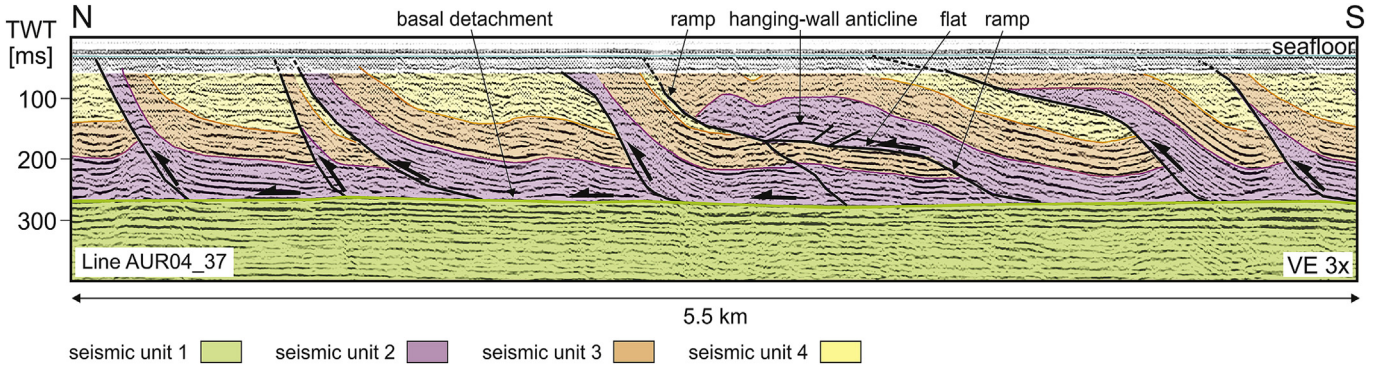

Fig. 2. Part of seismic section AUR04_37, showing southward dipping thrust-faults, along which sediment packages have been transported up to 1500 m along section. Note the detachment surface under which the strata are undeformed. The upper 20–50 ms is obstructed by noise and multiples. This detachment surface may have developed at the boundary between Upper Miocene fine-grained shelf/pro-delta deposits (green, seismic unit 1) and coarser-grained Upper Miocene delta-front deposits (violet, seismic unit 2). Seismic unit 3 (orange) probably represents uppermost Tortonian delta-front deposits, overlain by Messinian delta front/delta plain deposits (yellow seismic unit 4). (For interpretation of the references to colour in this figure legend, the reader is referred to the Web version of this article.)

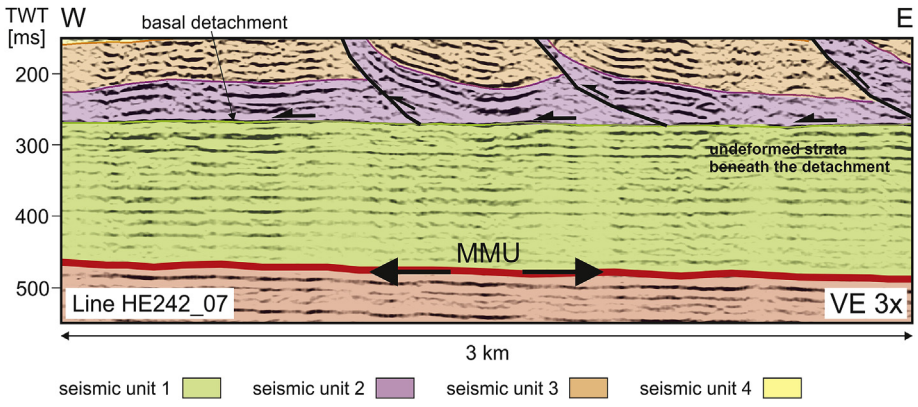

Fig. 3. Part of seismic section HE242_07. Below the detachment surface, there is a section of undisturbed strata showing low reflectivity (seismic unit 1, green). This zone is followed by a prominent reflector, which represents the Mid-Miocene Unconformity (MMU) (cf. Thöle et al., 2014). (For interpretation of the references to colour in this figure legend, the reader is referred to the Web version of this article.)

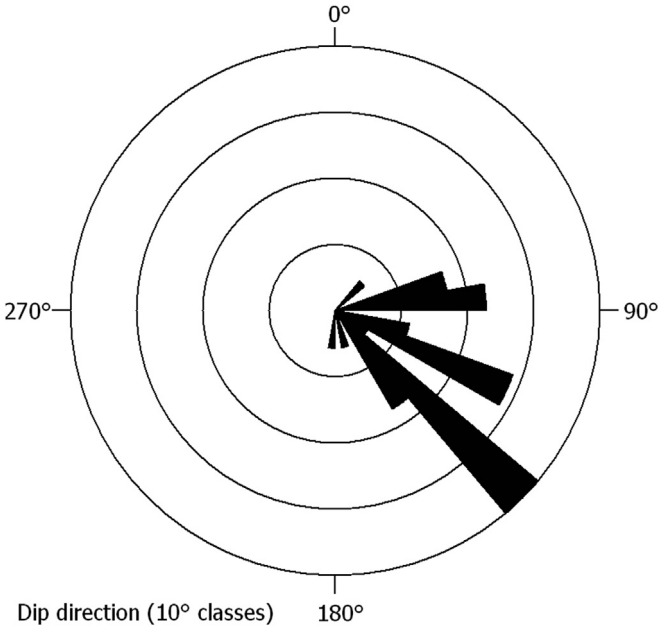

Fig. 4. Rose diagram showing the calculated dip directions of the thrust faults based on measurements on eight composite seismic sections (n = 28). Dips are towards SE, ESE and ENE, meaning the ice-push direction of D1 was towards NW to WSW.

(McClay, 1992; Tanner et al., 2010). Some of these triangle zones, however, are in the middle of the thrust-fault complex, and, as such, may represent snapshots of the progressive deformation (cf. Tanner et al., 2010).

4.1.3. Tunnel valleys

The glaciotectonic complex is bounded and incised by tunnel valleys (Figs. 1C and 5A), which are characterised by internal chaotic reflection patterns with sharp boundaries to the underlying and adjacent strata. On the western side of the glaciotectonic complex, a single tunnel valley can be mapped along the margin for more than 10 km. This tunnel valley strikes approximately northeast-southwest, is approximately 2 km wide and has a maximum depth of approximately 300 ms (TWT) (or 240 m).

The tunnel valley that incises the southern glaciotectonic complex has a similar depth; it is approximately 1.2 km wide and truncates the detachment surface (Figs. 1C and 5A). The strike direction of this tunnel valley is difficult to estimate, because it is only recorded on two seismic lines. Within the fill of this tunnel valley, pronounced deformation can be observed in the seismic sections. Two opposing fault-propagation folds are developed above new, steeply-dipping, slightly listric to listric reverse faults. Because these two fault-propagation folds are developed back to back, they form a pop-up structure. We attribute this deformation of the tunnel-valley fill to a younger ice advance from the East (deformation phase D3, see Discussion).

On the eastern side of the glaciotectonic complex, three generations of tunnel valleys occur (Fig. 1C). The oldest, deepest tunnel valleys strike northeast-southwest. These tunnel valleys are cut by two younger generations of tunnel valleys, which strike approximately east-west. These east-west striking tunnel valleys are 1–3.5 km wide and have depths of 100–150 ms (TWT) (80–120 m).

4.2. Interpretation of echosounder data

Echosounder data were used to image the shallow subsurface. The large glaciotectonic thrust-fault complex has no morphological expression at the sea floor. We do not know whether it reaches the sea-floor, because the uppermost part of the seismic profiles is distorted by noise and seabed multiples. The echosounder data and sampled near-surface sediments imply that the thrust-fault complex is overlain by coarse-grained reworked till and meltwater deposits of the Saalian Drenthe glaciation and fine-grained Holocene marine deposits (Figge, 1983; Neben, 2006; Coughlan et al., 2018). However, the echosounder data also reveal westward-dipping thrust faults (e.g., line HE 242-06) above the westernmost tunnel-valley fill that bounds the glaciotectonic complex (Figs. 1C and 6). We interpret the structure seen in the echosounder data as the hanging-wall of a ramp that passes into a flat at ca. 22 ms TWT (ca.13 m below seabed). The hanging-wall beds show fold-bend folding (Brandes and Tanner, 2014). The thrust apparently dips to the west in this 2D section, but the true dip direction could be to the Southwest or Northwest as well. The shallow thrust faults are covered by a thin layer of Holocene sediments (Fig. 6; Neben, 2006). We attribute this deformation, based on its orientation, location and depth, to the first Saalian Drenthe ice advance from the Northwest (deformation phase 2; see Discussion).

4.3. Kinematic restoration

Shortening results from the restoration of the D1 thrusts are also minimum values because of how the sections were constructed. Five profiles (AUR03_27, AUR04_30, AUR04_27, HE242_05, HE242_09) were restored to cover the most deformed part of the glaciotectonic complex. Two exemplary sections (AUR03_27 and AUR04_37) are discussed in more detail below (Fig. 7).

The deformed part of seismic section AUR03_27 has a post-deformation length of 14.7 km, and a restored length of 18.9 km, indicating shortening of 4.2 km or 22% (Fig. 7A). The section consists of 20 faults that dip in the same direction on the whole section. Offsets marginally increase eastwards as does the density of faults. Large offset values of up to 498 m are observed. Offset values decrease to the west on the five most-eastern faults. On the eastern side of the section, closely-spaced faults form imbricate stacks.

AUR04_37 is of great importance for the interpretation of the data, as it is one of only three north-south seismic sections that were affected by deformation. Although there is considerable variation in shortening within the section, no prominent trend can be recognized, although a slight decrease in deformation towards the south can be seen. Cross points of the north-south striking sections and west-east striking sections allow the reconstruction of true dip angles, as well as correlation of the faults and horizons. The most deformed north-south seismic section shows a number of interesting features when restored. The 13.7 km long AUR04_37 section was restored to an undeformed length of 20.9 km (Fig. 7B). 19 faults along the section are responsible for a total shortening of 6.9 km or 34%. Two adjacent faults alone account for 25% of the total shortening. Both show a typical flat-ramp-flat geometry within a system of duplex thrust-faults (cf. McClay, 1992). These large offset faults are likely to be the same thrust planes that are responsible for a large portion of offset on the eastern end of section HE242_09, as they are proximal to the crosspoint of the sections. In general, the amount of shortening decreases southward from the west-east profiles at 25%, through section HE242_09 to section AUR04_30 at 16% (for location, see Fig. 1B).

5. Discussion

5.1. Deformation events

The seismic and echosounder interpretation reveals that the glaciotectonic complex was affected by at least three deformation

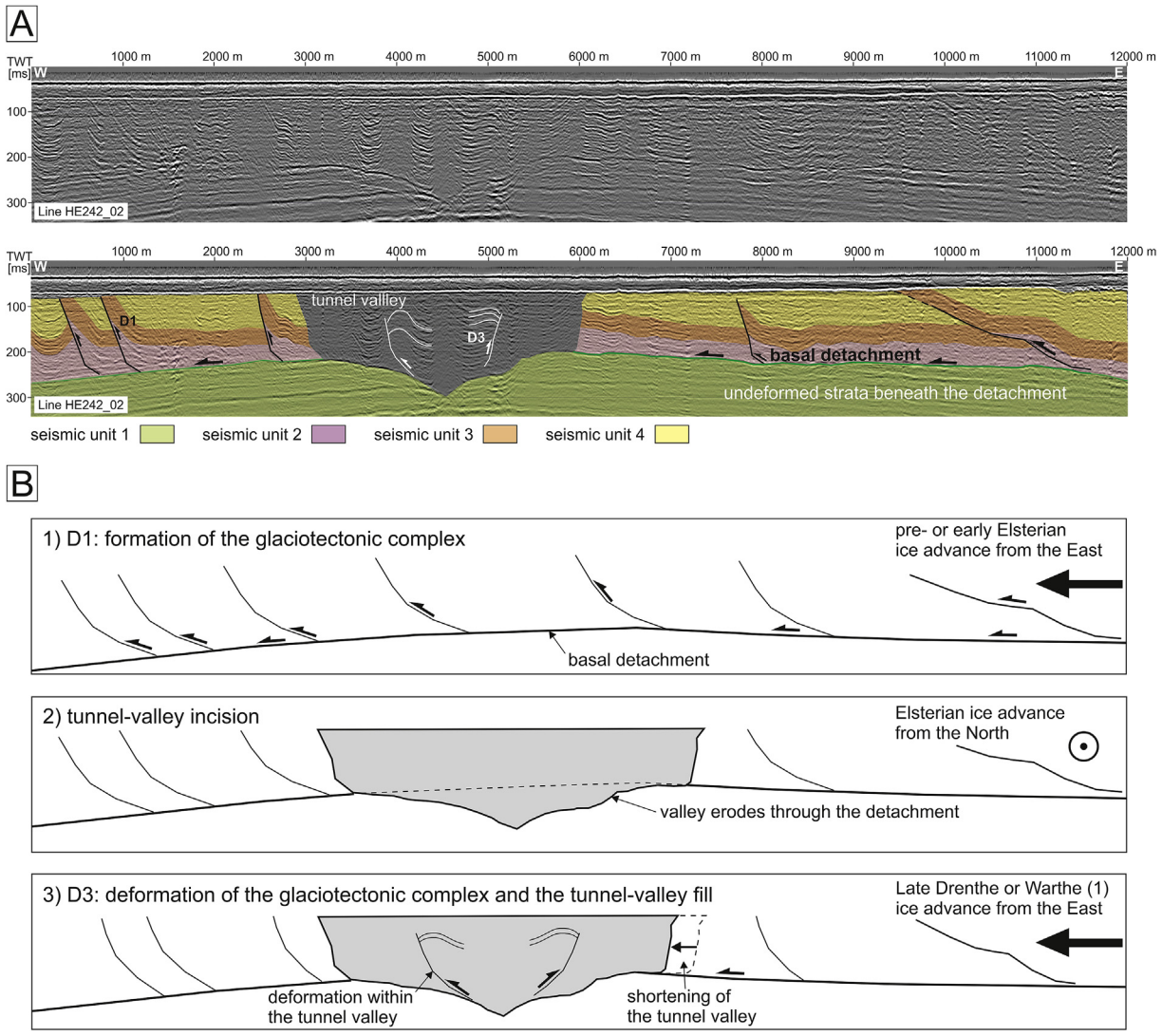

Fig. 5. Inferred deformation phases of the glaciotectonic complex of Heligoland. A) Part of seismic section HE242_02. B) Schematic evolution of the glaciotectonic deformation. During a pre- or and early Elsterian ice advance from the Baltic area, the Heligoland glaciotectonic thrust-fault complex formed (D1). Subsequently, a deep tunnel valley was incised into the glaciotectonic complex during an Elsterian ice advance from the North. During the Saalian late Drenthe or Warthe 1 ice advance the glaciotectonic complex and tunnel-valley fill underwent further shortening (deformation phase D3).

phases (D1-D3).

5.1.1. Deformation event D1

The first deformation, D1, is revealed by the seismic data. It is characterised by in-sequence thrusting above the basal detachment. Restoration of the five sections reveals more shortening on the N–S striking profile than on W-E striking profiles. The calculated shortening of 50% on section AUR04_37 (vs. values from as low as 16% up to 34% on the W-E profiles) imply that the N–S profiles are closer to true thrust direction than the W-E profiles. This is in agreement with the derived true fault plane dip towards SE and indicates the push direction towards the NW (Figs. 1D, 4 and 8A). The amount of shortening observed on the sections is between 16% and 34%; the average shortening is 23%. The amount of shortening of the Heligoland complex is comparable to other glaciotectonic complexes where shortening is in a range of 5–62.5% (Klint and Pedersen, 1995; Pedersen, 1996, 2005; Harris et al., 1997; Huuse and Lykke-Andersen, 2000b; Andersen, 2004). This similarity is likely driven by the structural style with a thin-skinned thrust fault deformation (Aber, 1982; Croot, 1987; Brandes and Le Heron, 2010; Cotterill et al., 2017; Vaughan-Hirsch and Phillips, 2017).

Apparent dip and plunge values were used to calculate true dip and plunge values (see section 3.3), following the method of Meissner and Stegena (1977). 28 dip values were measured from eight composite depth-converted sections. The true dip direction is towards the southeast or east-southeast direction (Fig. 4). We suggest therefore that the main compressive horizontal stress, indicating the ice movement, was towards the Northwest.

Borth-Hoffmann (1980) and Figge (1983), who first described the glaciotectonic complex north of Heligoland based on single-channel seismic data, interpreted similar directions derived from northwest-southeast and west-east section crosspoints, implying that directions presented above are true for the subsurface in this area and can be considered relevant for paleostress orientation analysis. The regional results of this study, in terms of ice advance and stress directions, are also in accordance with the findings of Borth-Hoffmann (1980). The major stress direction imposed on the sediments pushed them to the Northwest, implying that the main force came from a southeasterly direction. Whether the

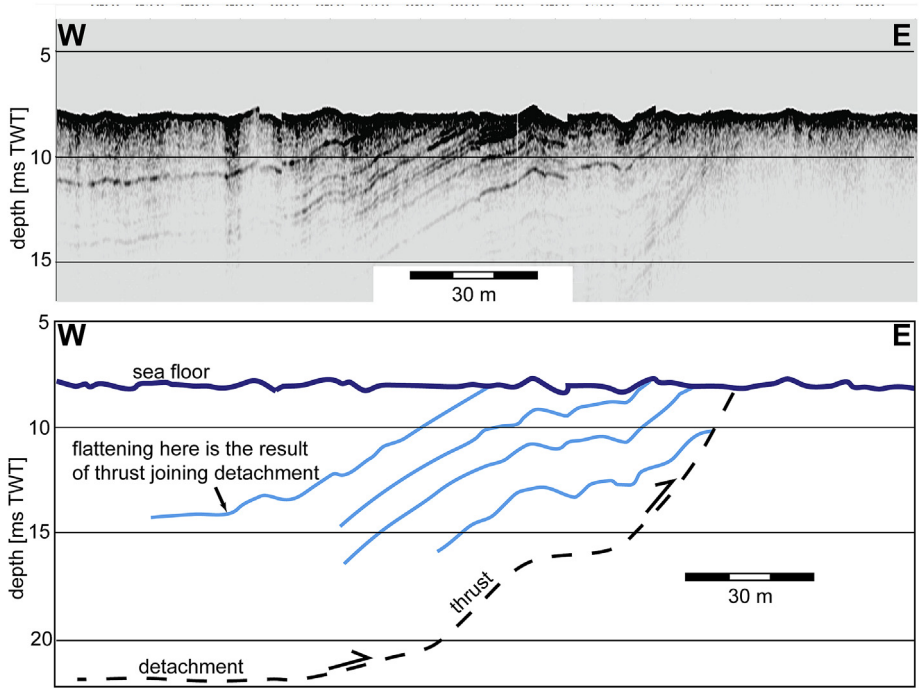

Fig. 6. Echosounder data (part of line HE242-06) showing westward-dipping thrust faults, overlain by a thin cover of fine-grained Holocene sediments. These shallow thrust faults probably formed during the first Saalian Drenthe ice-advance from the Northwest (deformation phase D2). The penetration depth is approximately 8 m (V_{sound} = 1500 m/s). For location, see Fig. 1C.

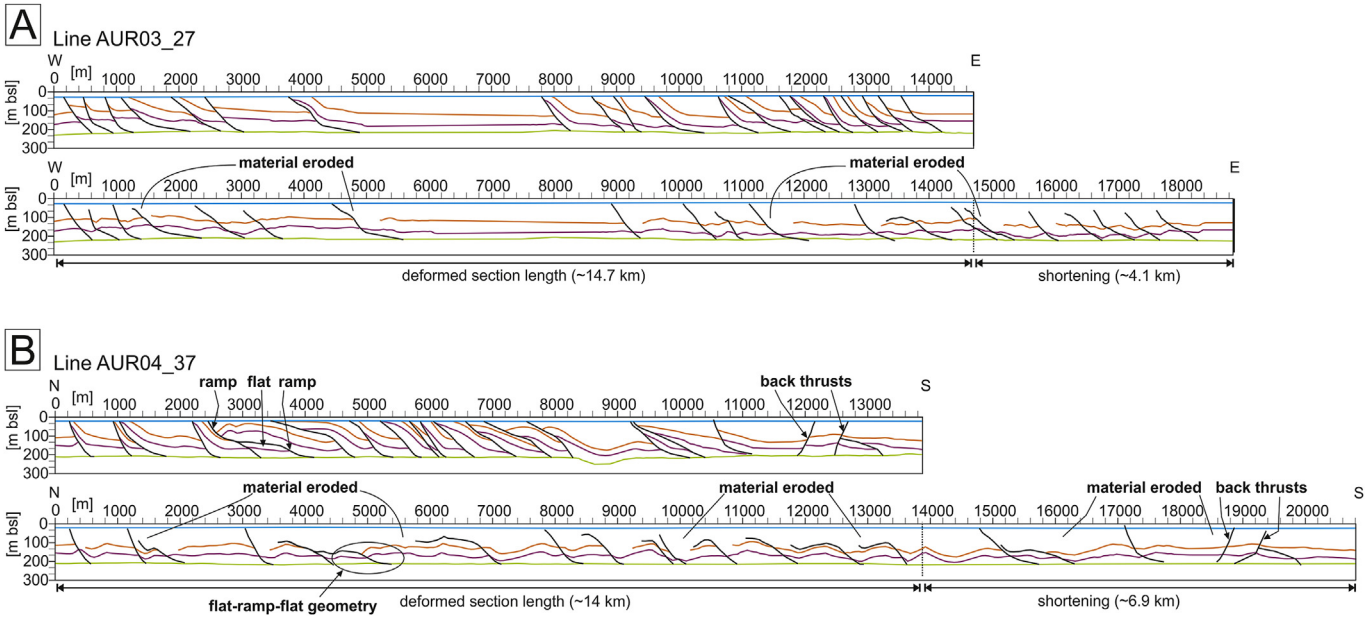

Fig. 7. Retro-deformation of seismic sections. A) Example of seismic section AUR04_27, showing the present-day section AUR03_27, interpreted from seismic data and the fully-restored section AUR03_27, with 4.1 km of shortening on 20 faults. It reveals a considerable amount of material loss due to erosion (white areas). Retro-deformation was started on the foreland-most, most-westerly fault. B) The present-day seismic section AUR04_37, interpreted from seismic data, and the fully-restored section AUR04_37, with 6.9 km of shortening on 19 faults. It also reveals a considerable amount of material loss due to erosion (white areas). Retro-deformation was started on the foreland-most, most-northerly fault.

glaciotectonic complex was caused by slow moving ice (e.g., Kälin, 1971), a surging ice-lobe (e.g., Vaughan-Hirsch and Phillips, 2017) or a fast-moving ice-stream, as discussed for the glaciotectonic complex in the Lower Rhine Embayment (e.g. Passchier et al., 2010; Lang et al., 2018), cannot be derived from the seismic data.

5.1.2. Tunnel valley incision

Subsequently, tunnel valleys were cut through the glaciotectonic complex, they even partly incised into the basal detachment (Fig. 5). For this reason, we postulate that the large northwest-southeast to northeast-southwest trending tunnel valleys are younger than the glaciotectonic complex (Fig. 8B).

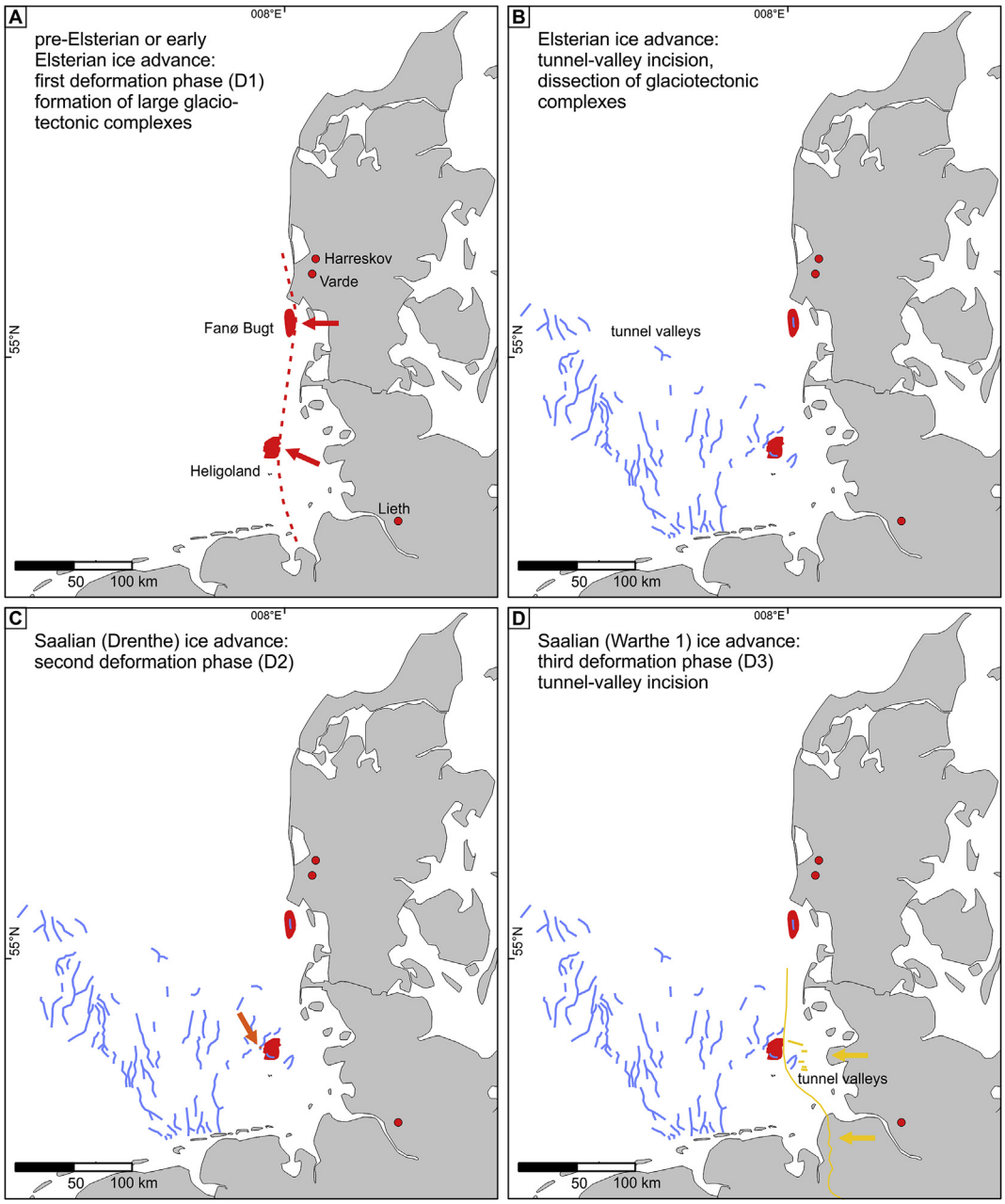

Fig. 8. Palaeogeographic maps showing the glacial history of the southeastern North Sea Basin. A) Formation of the Heligoland (and Fanø bugt?) glaciotectonic complexes during a pre- or early Elsterian ice advance from the East (deformation phase D1). B) Incision of deep tunnel valleys during a subsequent ice advance from the North (only tunnel valleys of the study area are shown). This ice advance may have occurred during either MIS 12 or MIS 10. C) Formation of shallow, westward-dipping thrusts (deformation stage D2) during the first Saalian Drenthe ice-advance from the Northwest (MIS 6). D) Formation of shallow east-west-trending tunnel valleys during the Saalian late Drenthe or Warthe 1 ice advance (only tunnel valleys of the study area are shown). Further shortening of the glaciotectonic complexes and deformation (D3) of the N–S trending Elsterian tunnel valleys that are incised into the glaciotectonic complex.

5.1.3. *Deformation events D2 and D3*

D2 deformation was recorded in the echosounder data (Fig. 6). It shows thrusting of the shallowest sediments, above a tunnel-valley fill (Fig. 1C). From the orientation of the thrusting, i.e. it most probably dips northwest or west, it may be due to the first Saalian Drenthe ice advance from the Northwest (Figs. 1D and 8C).

Later, a third deformation phase, D3, occurred, which caused the pre-existing glaciotectonic complex to undergo further shortening (Fig. 8D). This deformation phase can be clearly derived from the deformed tunnel-valley fills (Fig. 5B) and is most probably related to the Saalian Warthe 1 ice advance from the East (Figs. 1D and 8D).

5.2. *Possible detachment styles*

The detachment plays an important role in the development and appearance of the thrust-fault complex. The single detachment surface (ca. 200–240 m depth), in which the thrust faults sole, is one of the most striking features of this area. In order to start movement along a detachment, rheological differences between the two layers are necessary. Such rheological differences may be caused by i) an intra-bedrock boundary; (ii) a boundary between bedrock and poorly-consolidated sediment; iii) intra-formational discontinuities in poorly-consolidated sediments; iv) a boundary

between the base of the permafrost and the unfrozen sediment/bedrock; v) a boundary within frozen sediment caused by ice-rich and ice-poor zones or zones rich in liquid pore water; vi) a boundary between permafrost and the active layer; viii) a combination of any of the above options (Astakhov et al., 1996; Etzelmüller et al., 1996; Boulton et al., 1999; Fitzsimons et al., 1999; Huuse and Lykke-Andersen, 2000b; Andersen, 2004; McBride et al., 2007; Hiemstra et al., 2007; Burke et al., 2009; Waller et al., 2009, 2012; Lee et al., 2013; Szuman et al., 2013; Vaughan-Hirsch and Phillips, 2017).

Major unconformities in the Cenozoic sedimentary succession of the southeastern North Sea Basin are i) the top of the Eocene; ii) the near-top of the Oligocene; iii) the Mid-Miocene unconformity (MMU) and iv) the base of the Quaternary (glacigenic) deposits, commonly characterised by abrupt variations in permeability and grain size (e.g. Huuse and Clausen, 2001; Moreau et al., 2012; Thöle et al., 2014; Steinmetz et al., 2015).

The Eocene to Mid-Miocene unconformities can be ruled out as potential detachment surfaces because they lie at much greater depths in the study area (>380 m). The base of the Quaternary (glacigenic) deposits is not imaged in the seismic data because the upper 20–50 ms are obstructed by noise and multiples. Because of the shallow depth, we also rule out this unconformity as a potential detachment surface. Therefore, also the boundary between permafrost and the active layer can be ruled out. A likely detachment surface could be the boundary between Upper Miocene fine-grained shelf/pro-delta deposits and coarser-grained Upper Miocene delta-front deposits (Fig. 3).

Approximately 80 km south and north of the Heligoland glaciotectonic complex, this unconformity lies at a depth of ca. 200–250 m (Steinmetz et al., 2015; Thöle et al., 2014), corresponding with the depth of the mapped detachment surface here.

Hubbert and Rubey (1959), Strayer et al. (2001), and Boulton et al. (2004) suggest that higher pore pressure and porewater flow in proglacial sediments reduces shear strength, weakening an already-incompetent zone and thus become of great importance in the initial development of a detachment surface (Andersen et al., 2005). This would imply that the detachment for the described complex can be assumed to be of an initially weak lithology (e.g., clay or an extensive sand sheet with overpressurized porewater), further weakened by increasing pore pressure under the load of the ice sheet. Especially porewater pressure is important for sub- and proglacial systems. Rapid ice-advance may have led to the overpressurizing of porewater within a laterally extensive sand sheet, promoting the formation of a major detachment surface at the base of the developing thrust-fault complex (e.g., Iverson et al., 1995; Boulton, 1996; Glasser et al., 2006; Lee et al., 2013; Vaughan-Hirsch and Phillips, 2017).

It is also possible that the base of the permafrost or a boundary within the frozen sediment controlled the location of the basal detachment. A relatively impermeable permafrost horizon can potentially lead to the formation of a zone of high pore pressure at the base of the frozen sediment (e.g., Boulton et al., 1999). The presence of liquid porewater or ice-rich and ice-poor zones within the frozen sediment may lead to differences in cohesive strength and mechanical properties (e.g., Astakhov et al., 1996; Etzelmüller et al., 1996; Fitzsimons et al., 1999; Szuman et al., 2013).

The modelling study of Graβmann et al. (2010) predicts maximum permafrost depths for the German North Sea sector of ca. 250 m for the Cromerian glaciations, ca. 350 m for the Elsterian glaciations and ca. 150 m for the Saalian glaciations, based on a calibrated basal heat flow of 50 mW/m^2 (cf. Graβmann et al., 2005). The increased heat flow over salt domes, present in large numbers in northern Germany and the North Sea Basin, leads to a reduction of the maximum permafrost depth by up to 100 m. An earlier study by Delisle et al. (2007) implied shallower permafrost depths of approximately 80–170 m with a reduction of the maximum permafrost depth above salt domes by up to 40 m. The differences in permafrost thickness between both models is due to different basal heat flow scenarios. Delisle et al. (2007) applied an uncalibrated heatflow of 75 mW/m2, which according to Graβmann et al. (2005) is too high.

The modelled permafrost depths for the Cromerian glaciation (Graβmann et al., 2010) would correspond with the depth of the detachment surface and therefore, permafrost in the glacier foreland may have played a role for the location of the detachment surface. However, it is likely that the permafrost depth was highly irregular because of the numerous salt structures present in the study area, and therefore it probably did not form a continuous subhorizontal layer, as is seen in our data.

5.3. Implications of the age of the glaciotectonic complex, ice-marginal configurations, and correlation with onshore data

In the absence of age dating, precise stratigraphic control cannot be presented for the structures investigated in this study. The glacitotectonic restoration of the Heligoland thrust-fold complex implies that the deformation took place during a westward to northwestward ice advance from the Baltic area. The glaciotectonic complex of Heligoland is bounded and incised by tunnel valleys that postdate thrusting. These northeast-southwest to northwest-southeast trending deep tunnel valleys (up to 250 m deep; Figs. 1C, 5 and 8), belong to a large system of tunnel valleys that are thought to be Elsterian in age (e.g., Kuster and Meyer, 1979; Lutz et al., 2009; Stackebrandt, 2009; Hepp et al., 2012; Lang et al., 2012; Janszen et al., 2013; Steinmetz et al., 2015; Coughlan et al., 2018). The reconstructed Elsterian ice advances in northern Germany and the southern North Sea Basin indicate paleo-ice flow directions from the North, followed by ice-advances from the Northeast, and eventually from the East, as is indicated by the clast composition of tills and the orientation and cross-cutting relationships of subglacial tunnel valleys (e.g., Meyer, 1987; Stackebrandt, 2009; Ehlers et al., 2011; Hepp et al., 2012; Stephan, 2014; Coughlan et al., 2018). This would imply a pre-Elsterian formation of the Heligoland glaciotectonic complex, if the large northwest-southeast to northeast-southwest trending tunnel valleys formed during MIS 12 (e.g., Ehlers et al., 2011; Böse et al., 2012; Mellett et al., 2019). Field evidence for a pre-Elsterian glaciation of Denmark and Northern Germany have been reported by e.g., Vinx et al. (1997), Ehlers et al. (2011), Houmark-Nielsen (2011) and Høyer et al. (2013) (Fig. 1D). These pre-Elsterian tills are characterised by erratic clasts from western Scandinavian source areas, pointing to ice-advances from the North or Northeast and not from the Baltic area (e.g., Kronborg, 1986; Meyer, 1991; Vinx et al., 1997; Stephan, 2014). However, these reconstructed ice advances, which are based only on the count of a few samples of (reworked) till, do not necessarily exclude deformation by a regional ice stream from the East, the flow lines of which might have deviated from the reconstructed overall ice advance directions in its terminal zone (e.g., Boulton et al., 2001; Stokes and Clark, 2001; Passchier et al., 2010; Lang et al., 2018).

If the large northeast-southwest to northwest-southeast trending tunnel-valley fills formed during MIS 10, as was traditionally assumed for the age of the Elsterian tunnel-valley fills in northern Germany (e.g., Litt et al., 2007), then the main D1 deformation of the Heligoland glaciotectonic complex most probably occurred during MIS 12. Absolute MIS 10 ages have been given for two tunnel-valley fills further south onshore (cf. Lang et al., 2012,

2015; Roskosch et al., 2015) and there is increasing evidence for an MIS 10 age of the Elsterian Peelo Formation in the Netherlands (pers. comm. F.S. Busschers; Lee et al., 2012).

Further evidence for an old pre- or early Elsterian age of the Heligoland thrust-fold complex is given by the chronospatial relationship with younger tunnel valleys in the eastern part of the study area. Here, the deep northeast-southwest striking tunnel-valley fills are overlain by two different generations of tunnel-valley fills that trend approximately east-west (Fig. 1C). These tunnel-valley fills are much shallower (80–100 m) and correlation with onshore data imply a Saalian late Drenthe and Warthe 1 age (Andersen, 2004; Larsen and Andersen, 2005; Ehlers et al., 2011; Houmark-Nielsen, 2011; Jørgensen and Sandersen, 2006; Stephan, 2014, 2019; Sandsersen and Jørgensen, 2017; Coughlan et al., 2018; Lang et al., 2018). It is commonly accepted that the Weichselian ice advances did not reach the study area and therefore a Weichselian age for these tunnel valleys can be excluded (Carr et al., 2006; Larsen et al., 2009; Hughes et al., 2016). The western termination of the youngest east-west trending tunnel-valley fills therefore probably indicates the minimum extent of the Saalian Warthe 1 ice-sheet (Fig. 1C and D), corresponding with regional ice flow patterns in Northern Germany (Ehlers and Stephan, 1983; Meyer, 1987; Van Gijssel, 1987; Stephan, 2019). The third deformation phase that affected the Heligoland thrust-fold complex led to faulting of the older Elsterian tunnel-valley fills and may be related to these younger late Drenthe or early Warthe 1 ice advances.

We cannot determine from our data whether the Heligoland glaciotectonic complex marks the maximum extent of a pre- or an early Elsterian ice advance into the southeastern North Sea Basin or reflects a longer stillstand position during active ice retreat. In previous studies, the lateral change of deformation style has been interpreted as a consequence of ice-marginal oscillation during active reteat (cf., Lee et al., 2013; Cotterill et al., 2017; Phillips et al., 2018; Mellett et al., 2019). The structural style of the Heligoland glaciotectonic complex is characterised by mostly equidistant planar and listric thrusts that dip eastwards. In some cases, flat-ramp-flat geometries are developed. All faults sole into a common detachment. Therefore, the structural style of Heligoland glaciotectonic complex does not show evidence of more complex ice-front oscillations. However, it must be kept in mind that the Heligoland glaciotectonic complex may only represent an erosional relic and we cannot rule out that the maximum extent of the ice-margin was located further west.

A similar chronospatial relationship between glaciotectonic complexes and large northeast-southwest to northwest-southeast striking tunnel valleys has been reported from the Fanø bugt complex, offshore northern Denmark (Fig. 1D). This large glaciotectonic complex shows different thrust directions that range from westerly, southerly to easterly directions, implying that the deformation was not coeval and belonged to different ice advances (Huuse and Lykke-Andersen, 2000b). Larsen and Andersen (2005) reported that the deformation of the Fanø bugt glaciotectonic complex involves Miocene and younger sediments including the Esbjerg Yoldia Clay, which is discordantly overlain by a till with a typical 'Baltic' composition. The Esbjerg Yoldia Clay was dated to the latest Elsterian-early Holsteinian by Knudsen and Penney (1987), therefore pointing to a Saalian (Drenthe and Warthe) deformation. However, amino acid measurements, performed on mollusc shells by Miller and Mangerud (1996), suggest that the Esbjerg Yoldia Clay may be older than the Elsterian. If this dating is correct, the age of the deformation may be partly older, corresponding to the findings of Huuse and Lykke-Andersen (2000b). The Fanø bugt and Jammerbugt glaciotectonic complexes are onlapped by Eemian and Weichselian deposits, giving a minimum age for the deformation (Andersen, 2004; Larsen and Andersen, 2005; Pedersen and Boldreel, 2017). This would also correspond to the Saalian deformation phase, recorded in the glaciotectonic complexes located further south onshore in northern Germany (Altenwalder and Lamstedt Moraine; Höfle and Lade, 1983; Meyer, 1987; Van Gijssel, 1987). We therefore assume that the large glaciotectonic complexes offshore western Denmark and Northern Germany have a long multiphase deformation history. The different orientations of glaciotectonic structures and their chronospatial relationships with tunnel-valley systems imply that these large glaciotectonic complexes formed during different (pre-)Elsterian to Warthian ice advances.

6. Conclusions

The glaciotectonic complex of Heligoland forms part of a large belt of glaciotectonic complexes that stretches from offshore Denmark via northern Germany to Poland. From 6500 km of high-resolution, multi-channel, 2-D seismic data obtained in the German Bight to the north of Heligoland, we describe the structure of this ca. 350 km^2 large glaciotectonic complex that consists mainly of Neogene delta deposits above a horizontal detachment at a depth of about 200 m–240 m.

By kinematically restoring five seismic sections, we determined the minimum shortening due to thrusting and folding. Shortening is much higher in north-south sections (ca. 50%) than in east-west striking sections (16–34%). Because the true dip of the faults is to the Southeast, we suggest the thrust complex was pushed west-to north-westwards. The average shortening is 23%, which is comparable to that obtained for other glaciotectonic structures.

The detachment surface most probably formed at a pronounced rheological boundary between Upper Miocene, fine-grained, shelf or pro-delta deposits and coarser-grained, delta-front deposits, although we cannot rule out that deep permafrost in the glacier foreland played a role in the location of this detachment surface.

The presence of deep, northwest-southeast to northeast-southwest trending Elsterian tunnel valleys that cross-cut or bound the glaciotectonic complex of Heligoland suggests that the glaciotectonic complex was produced during a pre-Elsterian (MIS 16?) or early Elsterian (MIS 12?) ice advance from easterly to southeasterly directions, depending on the age of the tunnel-valleys (MIS 12 or MIS 10?).

A second deformation phase occurred during a subsequent Saalian Drenthe ice advance from the Northwest, as is indicated by the occurrence of shallow, westward-dipping thrust faults that were recorded in the echosounder data.

During a third deformation phase, the glaciotectonic complex underwent further shortening with deformation of the tunnel-valley fill by fault-propagation folding in opposing directions. This deformation phase may have occurred during the Saalian late Drenthe or Warthe 1 ice advances, corresponding to the Saalian deformation of glaciotectonic complexes, located further north offshore Denmark and further south onshore in northern Germany.

The restoration of the glaciotectonic complex of Heligoland and its chronospatial relationship with Elsterian and Saalian tunnel valleys implies that the glaciotectonic complexes offshore Denmark and northern Germany has a complex history and probably formed during different (pre-)Elsterian to Warthian ice advances. Whether these glaciotectonic complexes were caused by slow moving ice, surging ice-lobes or a fast-moving ice-stream, cannot be determined from the data.

Based on the integration of palaeo-ice flow data derived from the glaciotectonic-thrust complex and mapped tunnel valleys and mega-scale glacial lineations, we present new palaeogeographic

reconstructions of previously unknown (pre-) Elsterian and Warthian ice-margins in the southeastern North Sea Basin.

Acknowledgments

The research presented in this paper was part of the Diploma Thesis of Hannes Koopmann carried out at the Federal Institute for Geosciences and Natural Resources (BGR) and Leibniz Universität Hannover. We thank crew members and participants of cruises BGR03, BGR04 and HE242, especially the party chiefs H. Kudraβ, S. Neben, L. Reinhardt and M. Wiedicke. We further thank reviewers, J. Lee and R. Waller as well as editor C. O'Cofaigh for insightful comments, which helped to improve this manuscript. F.S. Busschers, A. Grube, P. Sandersen and H.-J. Stephan are thanked for discussion. The authors acknowledge the use of the MOVE Software Suite granted by Petroleum Experts Limited, which we used to restore the cross-sections.

References

Aber, J.S., 1982. Model for glaciotectonism. Bull. Geol. Soc. Den. 30, 79–90.
Aber, J.S., Ber, A., 2007. Glaciotectonism. Devel. Quat. Sci. 6, 1–246.
Andersen, L.T., 2004. The Fanø Bugt Glaciotectonic Thrust Fault Complex, Southeastern Danish North Sea. A Study of Large-Scale Glaciotectonics Using High-Resolution Seismic Data and Numerical Modelling. Ph.D.-thesis. University of Aarhus, Denmark.
Andersen, L.T., Hansen, D.L., Huuse, M., 2005. Numerical modelling of thrust structures in unconsolidated sediments: implications for glaciotectonic deformation. J. Struct. Geol. 27, 587–596.
Arfai, J., Jähne, F., Lutz, R., Franke, D., Gaedicke, C., Kley, J., 2014. Late Palaeozoic to early Cenozoic geological evolution of the northwestern German North Sea (Entenschnabel): new results and insights. Neth. J. Geosci. 93, 147–174.
Arfai, J., Franke, D., Lutz, R., Reinhardt, L., Kley, J., Gaedicke, C., 2018. Rapid quaternary subsidence in the northwestern German North Sea. Sci. Rep. 8, 11524.
Astakhov, V.I., Kaplyanskaya, F.A., Tarnogradsky, V.D., 1996. Pleistocene permafrost of West Siberia as a deformable glacier bed. Permafr. Periglac. Process. 7, 165–191.
Beets, D.J., Meijer, T., Beets, C.J., Cleveringa, P., Laban, C., Van der Spek, A.J.F., 2005. Evidence for a middle Pleistocene glaciation of MIS 8 age in the southern North sea. Quat. Int. 133, 7–19.
Bendixen, C., Lamb, R.M., Huuse, M., Boldreel, L.O., Jensen, J.B., Clausen, O.R., 2018. Evidence for a grounded ice sheet in the Central North sea during the early middle Pleistocene Donian glaciation. J. Geol. Soc. 175, 291–307.
Bennett, M.R., 2001. The morphology, structural evolution and significance of push moraines. Earth Sci. Rev. 53, 197–236.
Bennett, M.R., Huddart, D., Waller, R.I., Midgley, N.G., Gonzalez, N., Tomio, N., 2004. Styles of ice-marginal deformation at Hagafellsjökull-Eystri, Iceland during the 1998/99 winter-spring surge. Boreas 33, 97–107.
Benvenuti, A., Šegvić, B., Moscariello, A., 2018. Tunnel valley deposits from the southern North Sea–material provenance and depositional processes. Boreas 47, 625–642.
Böse, M., Lüthgens, C., Lee, J.R., Rose, J., 2012. Quaternary glaciations of northern Europe. Quat. Sci. Rev. 44, 1–25.
Borth-Hoffmann, B., 1980. Flachseismische Untersuchung geologischer Strukturen in der östlichen Deutschen Bucht. Diploma thesis. University of Kiel, Germany.
Boulton, G.S., 1996. Theory of glacial erosion, transport and deposition as a consequence of subglacial sediment deformation. J. Glaciol. 42, 43–62.
Boulton, G.S., van der Meer, J.J.M., Beets, D.J., Hart, J.K., Ruegg, G.H.J., 1999. The sedimentary and structural evolution of a recent push moraine complex: Holmstrømbreen, Spitsbergen. Quat. Sci. Rev. 18, 339–371.
Boulton, G.S., Dongelmans, P., Punkari, M., Broadgate, M., 2001. Palaeoglaciology of an ice sheet through a glacial cycle: the European ice sheet through the Weichselian. Quat. Sci. Rev. 20, 591–625.
Boulton, G.S., van der Meer, J.J.M., Beets, D.J., Hart, J.K., Ruegg, G.H.J., 2004. The sedimentary and structural evolution of a recent push moraine complex: Holmströmbreen, Spitsbergen. Dev. Quat. Sci. 4, 149–180.
Brandes, C., Le Heron, D.P., 2010. The glaciotectonic deformation of Quaternary sediments by fault-propagation folding. Proc. Geol. Assoc. 121, 270–280.
Brandes, C., Tanner, D.C., 2014. Fault-related folding: a review of kinematic models and their application. Earth Sci. Rev. 138, 352–370.
Buckley, F.A., 2017. A glaciogenic sequence from the Early Pleistocene oft he central North Sea. J. Quat. Sci. 32, 145–168.
Burke, H., Phillips, E., Lee, J.R., Wilkinson, I.P., 2009. Imbricate thrust stack model for the formation of glaciotectonic rafts: an example from the Middle Pleistocene of north Norfolk, UK. Boreas 38, 620–637.
Busschers, F.S., van Balen, R.T., Cohen, K.M., Kasse, C., Weerts, H.J.T., Wallinga, J., Bunnik, F.P.M., 2008. Response of the Rhine-Meuse fluvial system to Saalian ice-sheet dynamics. Boreas 37, 377–398.
Cameron, T.D.J., Bulat, J., Mesdag, C.S., 1993. High resolution seismic profile through a Late Cenozoic delta complex in the southern North Sea. Mar. Pet. Geol. 10, 591–599.
Carr, S.J., Holmes, R., van der Meer, J.J.M., Rose, J., 2006. The last glacial maximum in the north Sea basin: micromorphological evidence of extensive glaciation. J. Quat. Sci. 21, 131–153.
Clark, C.D., 1993. Mega-scale glacial lineations and cross-cutting ice-flow landforms. Earth Surf. Process. Landforms 18, 1–29.
Cohen, K.M., Gibbard, P.L., Weerts, H.J.T., 2014. North Sea palaeogeographical reconstructions for the last 1 Ma. Neth. J. Geosci. 93, 7–29.
Cohen, K.M., Westley, K., Erkens, G., Hijma, M.P., Weerts, H.J., 2017. The North Sea. In: Flemming, N.C., Harff, J., Moura, D., Burgess, A., Bailey, G.N. (Eds.), Submerged Landscapes of the European Continental Shelf. Wiley & Sons, Chichester, pp. 147–186.
Cotterill, C.J., Phillips, E., James, L., Forsberg, C.F., Tjelta, T.I., Carter, G., Dove, D., 2017. The evolution of the Dogger Bank, North Sea: a complex history of terrestrial, glacial and marine environmental change. Quat. Sci. Rev. 171, 136–153.
Coughlan, M., Fleischer, M., Wheeler, A.J., Hepp, D.A., Hebbeln, D., Mörz, T., 2018. A revised stratigraphical framework for the Quaternary deposits of the German North Sea sector: a geological-geotechnical approach. Boreas 47, 80–105.
Croot, D.G., 1987. Glacio-tectonic structures: a mesoscale model of thin-skinned thrust sheets? J. Struct. Geol. 9, 797–808.
Croot, D.G., 1988. Glaciotectonics and surging glaciers: a correlation based on Vestspitsbergen Svalbard, Norway. In: Croot, D.G. (Ed.), Glaciotectonics: Forms and Processes. Balkema, Rotterdam, pp. 49–61.
Deckers, J., Louwye, S., 2019. Late Miocene increase in sediment accommodation rates in the southern North Sea Basin. Geol. J. https://doi.org/10.1002/gj.3438.
Delisle, G., Graßmann, S., Cramer, B., Messner, J., Winsemann, J., 2007. Estimating episodic permafrost development in northern Germany during the Pleistocene. In: Hambrey, M., Christoffersen, P., Glasser, N., Hubbard, B. (Eds.), Glacial Processes and Products, vol. 39. Spec. Publs. Int. Ass. Sediment., pp. 109–119
Dobrowolski, R., Terpilowski, S., 2006. Influence of palaeokarst morphology on the formation of ice-pushed ridges: a case study from Rejowiec, eastern Poland. Boreas 35, 213–221.
Dove, D., Evans, D.J.A., Lee, J.R., Roberts, D.H., Tappin, D.R., Mellett, C.L., Long, D., Callard, S.L., 2017. Phased occupation and retreat of the last British–Irish Ice Sheet in the southern North Sea; geomorphic and seismostratigraphic evidence of a dynamic ice lobe. Quat. Sci. Rev. 163, 114–134.
Ehlers, J., Stephan, H.-J., 1983. Till fabric and ice-movement. In: Ehlers, J. (Ed.), Glacial Deposits in North-west Europe. Balkema, Rotterdam, pp. 267–274.
Ehlers, J., Grube, A., Stephan, H.J., Wansa, S., 2011. Chapter 13 – Pleistocene glaciations of north Germany - new results. In: Ehlers, J., Gibbard, P.L., Hughes, P.D. (Eds.), Quaternary Glaciations - Extent and Chronology – A Closer Look. Develop. Quat. Sci., vol. 15, pp. 149–162.
Etzelmüller, B., Hagen, J.O., Vatne, G., Ødegård, R.S., Sollid, J.L., 1996. Glacier debris accumulation and sediment deformation influenced by permafrost: examples from Svalbard. Ann. Glaciol. 22, 53–62.
Feeser, V., 1988. On the mechanics of glaciotectonic contortion of clays. In: Croot, D.G. (Ed.), Glaciotectonics: Forms and Processes. Balkema, Rotterdam, pp. 63–76.
Figge, K., 1983. Morainic deposits in the German Bight area of the north sea. In: Ehlers, J. (Ed.), Glacial Deposits in North-West Europe. Balkema, Rotterdam, pp. 299–304.
Fitzsimons, S.J., McManus, K.J., Lorrain, R.D., 1999. Structure and strength of basal ice and substrate of a dry-based glacier: evidence for substrate deformation at sub-freezing temperatures. Ann. Glaciol. 28, 236–240.
Gehrmann, A., Harding, C., 2018. Geomorphological mapping and spatial analyses of an Upper Weichselian glacitectonic complex based on LiDAR data, Jasmund Peninsula (NE Rügen), Germany. Geosciences 8 (6), 208.
Gibbard, P.L., Lewin, J., 2009. River incision and terrace formation in the late Cenozoic of Europe. Tectonophys 474, 41–55.
Gibbard, P.L., Lewin, J., 2016. Filling the north Sea basin: Cenozoic sediment sources and river styles (André Dumont medallist lecture 2014). Geol. Belg. 19, 1–17.
Gibbons, A.B., Megeath, J.D., Pierce, K.L., 1984. Probability of moraine survival in a succession of glacial advances. Geology 12, 327–330.
Glasser, N.F., Jansson, K., Mitchell, W.A., Harrison, S., 2006. The geomorphology and sedimentology of the 'Témpanos' moraine at Laguna San Rafael, Chile. J. Quat. Sci. 21, 629–643.
Graham, A.G., Stoker, M.S., Lonergan, L., Bradwell, T., Stewart, M.A., 2011. The Pleistocene glaciations of the north Sea basin. In: Ehlers, J., Gibbard, P.L., Hughes, P.D. (Eds.), Quaternary Glaciations - Extent and Chronology – A Closer Look. Develop. Quat. Sci., vol. 15, pp. 261–278.
Gramann, F., 1989. Forschungsbohrung Wursterheide. Benthonische Foraminiferen und verwandte Mikrofossilien. Biostratigraphie, Faziesanalyse. Geol. J. A111, 287–319.
Graßmann, S., Cramer, B., Delisle, G., Messner, J., Winsemann, J., 2005. Geological history and petroleum system of the Mittelplate oil field, Northern Germany. Int. J. Earth Sci. 94, 979–989.
Graßmann, S., Cramer, B., Delisle, G., Hantschel, T., Messner, J., Winsemann, J., 2010. pT-effects of Pleistocene glacial periods on permafrost, gas hydrate stability zones and reservoir of the Mittelplate oil field, northern Germany. Mar. Pet. Geol. 27, 298–306.
Harris, C., Williams, G., Bramham, P., Eaton, G., McCarroll, D., 1997. Glaciotectonized quaternary sediments at Dinas Dinlle, Gwynedd, north Wales, and their bearing on the style of deglaciation in the eastern Irish sea. Quat. Sci. Rev. 16, 109–127.
Hepp, D.A., Hebbeln, D., Kreiter, S., Keil, H., Bathmann, C., Ehlers, J., Mörz, T., 2012.

An east–west-trending Quaternary tunnel valley in the south-eastern North Sea and its seismic–sedimentological interpretation. J. Quat. Sci. 27, 844–853.
Hiemstra, J.F., Evans, D.J.A., Ó Cofaigh, C., 2007. The role of glacitectonic rafting and comminution in the production of subglacial tills: examples from southwest Ireland and Antarctica. Boreas 36, 386–399.
Höfle, H.C., Lade, U., 1983. The stratigraphic position of the Lamstedter moraine within the younger Drenthe substage (middle Saalian). In: Ehlers, J. (Ed.), Glacial Deposits in North-West Europe. Balkema, Rotterdam, pp. 343–346.
Houmark-Nielsen, M., 2011. Chapter 5-Pleistocene glaciations in Denmark: a closer Look at Chronology, ice dynamics and landforms. In: Ehlers, J., Gibbard, P.L., Hughes, P.D. (Eds.), Quaternary Glaciations - Extent and Chronology – A Closer Look. Develop. Quat. Sci., vol. 15, pp. 47–58.
Høyer, A.S., Jørgensen, F., Piotrowski, J.A., Jakobsen, P.R., 2013. Deeply rooted glaciotectonism in western Denmark: geological composition, structural characteristics and the origin of Varde hill-island. J. Quat. Sci. 28, 683–696.
Hubbert, M.K., Rubey, W.W., 1959. Role of fluid pressure in mechanics of overthrust faulting. Bull. Geol. Soc. Am. 70, 115–166.
Hughes, A.L., Gyllencreutz, R., Lohne, Ø.S., Mangerud, J., Svendsen, J.I., 2016. The last Eurasian ice sheets–a chronological database and time-slice reconstruction, DATED-1. Boreas 45, 1–45.
Huuse, M., Lykke-Andersen, H., 2000a. Overdeepened Quaternary valleys in the eastern Danish North Sea: morphology and origin. Quat. Sci. Rev. 19, 1233–1253.
Huuse, M., Lykke-Andersen, H., 2000b. Large-scale glaciotectonic thrust structures in the eastern Danish North Sea. In: Maltman, A.J., Hubbard, B., Hambrey, M.J. (Eds.), Deformation of Glacial Materials, vol. 176. Geol. Soc. Lond. Spec. Publ., pp. 293–305
Huuse, M., Clausen, O.R., 2001. Morphology and origin of major Cenozoic sequence boundaries in the eastern North Sea Basin: top Eocene, near-top Oligocene and the mid-Miocene unconformity. Basin Res. 13, 17–41.
Ingólfsson, O., 1988. Large-scale glaciotectonic deformation of soft sediments: a case study of a late Weichselian sequence in western Iceland. In: Croot, D.G. (Ed.), Glaciotectonics: Forms and Processes. Balkema, Rotterdam, pp. 101–107.
Iverson, N.R., Hanson, B., Hooke, R.L., Jansson, P., 1995. Flow mechanism of glaciers on soft beds. Science 267 (5194), 80–81.
Janszen, A., Moreau, J., Moscariello, A., Ehlers, J., Kröger, J., 2013. Time-transgressive tunnel-valley infill revealed by a three-dimensional sedimentary model, Hamburg, north-west Germany. Sedimentology 60, 693–719.
Jørgensen, F., Piotrowski, J.A., 2003. Signature of the Baltic ice stream on Funen island, Denmark during the Weichselian glaciation. Boreas 32, 242–255.
Jørgensen, F., Sandersen, P.B.E., 2006. Buried and open tunnel valleys in Denmark – erosion beneath multiple ice sheets. Quat. Sci. Rev. 25, 1339–1363.
Kälin, M., 1971. Doctoral thesis No. 4671 The Active Push Moraine of the Thompson Glacier, Axel Heiberg Island, Canadian Arctic Archipelago, Canada. ETH Zürich, Switzerland.
Kehew, A.E., Piotrowski, J.A., Jørgensen, F., 2012. Tunnel valleys: Concepts and controversies - a review. Earth Sci. Rev. 113, 33–58.
Kjær, K.H., Houmark-Nielsen, M., Richardt, N., 2003. Ice-flow patterns and dispersal of erratics at the southwestern margin of the last Scandinavian Ice Sheet: signature of palaeo-ice streams. Boreas 32, 130–148.
Klint, K.E.S., Pedersen, S.A.S., 1995. The Hanklit glaciotectonic thrust fault complex, Mors, Denmark. Dan. Geol. Undersøg 35, 1–30.
Knudsen, K.L., Penney, D.N., 1987. Foraminifera and Ostracoda in Late Elsterian-Holsteinian Deposits at Tornskov and Adjacent Areas in Jutland, Denmark. Dan. Geol. Undersøg, Miljøministeriet, København.
Knox, R.W.O.B., Bosch, J.H.A., Rasmussen, E.S., Heilmann-Clausen, C., Hiss, M., De Lugt, I.R., Kasiński, J., King, C., Köthe, A., Słodkowska, B., Standke, G., Vandenberghe, N., 2010. In: Doornenbal, J.C., Stevenson, A.G. (Eds.), Petroleum Geological Atlas of the Southern Permian Basin Area. EAGE Publications, Housten, pp. 211–223. Cenozoic.
Köthe, A., 2012. A revised Cenozoic dinoflagellate cyst and calcareous nannoplankton zonation for the German sector of the southeastern North Sea Basin. Newsl. Stratigr. 45, 189–220.
Kowalski, A., Makoś, M., Pitura, M., 2019. New insights into the glacial history of southwestern Poland based on large-scale glaciotectonic deformations–a case study from the Czaple II Gravel Pit (Western Sudetes). Ann. Soc. Geol. Pol. 88, 341–359.
Kristensen, T.B., Huuse, M., Piotrowski, J.A., Clausen, O.R., 2007. A morphometric analysis of tunnel valleys in the eastern North Sea based on 3D seismic data. J. Quat. Sci. 22, 801–815.
Kronborg, C., 1986. Fine gravel contents of till. In: Møller, J.T. (Ed.), Twentyfive Years of Geology. Aarhus Geoskrifter, vol. 24, pp. 189–210.
Kudraß, H.S., (party chief) with contributions by the shipboard scientific party, 2003. Fahrtbericht/Cruise Report MV Aurelia Cruise BGR03-AUR–Nordsee–16.09.2003–09.10.2003. Unpublished. Bundesanstalt für Geowissenschaften und Rohstoffe, Hannover.
Kuhlmann, G., de Boer, P., Pedersen, R.B., Wong, Th.E., 2004. Provenance of Pliocene sediments and paleoenvironmental changes in the southern North Sea region using Samarium-Neodymium (Sm/Nd) provenance ages and clay mineralogy. Sediment. Geol. 171, 205–226.
Kuster, H., 2005. Das jüngere Tertiär in Nord- und Nordostniedersachsen. Geol. J. A158, 1–194.
Kuster, H., Meyer, K.-D., 1979. Glaziäre Rinnen im mittleren und nordöstlichen Niedersachsen. Eiszeitalt. Ggw. 29, 135–156.
Laban, C., van der Meer, J.J., 2011. Pleistocene glaciation in The Netherlands. In: Ehlers, J., Gibbard, P.L., Hughes, P.D. (Eds.), Quaternary Glaciations – Extent and Chronology – A Closer Look. Develop. Quat. Sci., vol. 15, pp. 247–260.
Lang, J., Winsemann, J., Steinmetz, D., Pollok, L., Polom, U., Böhner, U., Serangeli, J., Brandes, C., Hampel, A., Winghart, S., 2012. The Pleistocene of Schöningen (Germany): a complex tunnel valley-fill revealed from 3D subsurface modelling (GOCAD) and shear-wave seismics. Quat. Sci. Rev. 39, 86–105.
Lang, J., Hampel, A., Brandes, C., Winsemann, J., 2014. Response of salt structures to ice-sheet loading: implications for ice-marginal and subglacial processes. Quat. Sci. Rev. 101, 217–233.
Lang, J., Böhner, U., Polom, U., Serangeli, J., Winsemann, J., 2015. The middle Pleistocene tunnel valley at Schöningen as a Paleolithic archive. J. Hum. Evol. 89, 18–26.
Lang, J., Lauer, T., Winsemann, J., 2018. New age constraints for the Saalian glaciation in northern central Europe: implications for the extent of ice sheets and related proglacial lake systems. Quat. Sci. Rev. 180, 240–259.
Lauer, T., Weiss, M., 2018. Timing of the Saalian-and Elsterian glacial cycles and the implications for Middle–Pleistocene hominin presence in central Europe. Sci. Rep. 8, 5111.
Larsen, B., Andersen, L.T., 2005. Late Quaternary stratigraphy and morphogenesis in the Danish eastern North Sea and its relation to onshore geology. Neth. J. Geosci. 84, 113–128.
Larsen, N.K., Knudsen, K.L., Krohn, C.F., Kronborg, C., Murray, A.S., Nielsen, O.B., 2009. Late Quaternary ice sheet, lake and sea history of southwest Scandinavia–a synthesis. Boreas 38, 732–761.
Lee, J.R., Phillips, E.R., 2008. Progressive soft sediment deformation within a subglacial shear zone—a hybrid mosaic–pervasive deformation model for Middle Pleistocene glaciotectonised sediments from eastern England. Quat. Sci. Rev. 27, 1350–1362.
Lee, J.R., Busschers, F.S., Sejrup, H.P., 2012. Pre-Weichselian Quaternary glaciations of the British Isles, The Netherlands, Norway and adjacent marine areas south of 68°N: implications for long-term ice sheet development in northern Europe. Quat. Sci. Rev. 44, 213–228.
Lee, J.R., Phillips, E., Booth, S.J., Rose, J., Jordan, H.M., Pawley, S.M., Warren, M., Lawley, R.S., 2013. A polyphase glacitectonic model for ice-marginal retreat and terminal moraine development: the Middle Pleistocene British Ice Sheet, northern Norfolk, UK. Proc. Geol. Assoc. 124, 753–777.
Lee, J.R., Phillips, E., Rose, J., Vaughan-Hirsch, D., 2017. The Middle Pleistocene glacial evolution of northern East Anglia, UK: a dynamic tectonostratigraphic–parasequence approach. J. Quat. Sci. 32, 231–260.
Litt, T., Behre, K.-E., Meyer, K.-D., Stephan, H.-J., Wansa, S., 2007. Stratigraphische Begriffe für das Quartär des norddeutschen Vereisungsgebietes. E G Quat. Sci. J. 56, 7–65.
Lonergan, L., Maidment, S.C., Collier, J.S., 2006. Pleistocene subglacial tunnel valleys in the central North Sea basin: 3-D morphology and evolution. J. Quat. Sci. 21, 891–903.
Lutz, R., Kalka, S., Gaedicke, C., Reinhardt, L., Winsemann, J., 2009. Pleistocene tunnel valleys in the German North Sea: spatial distribution and morphology. Z. Deut. Ges. Geow 160, 225–235.
Madsen, T.M., Piotrowski, J.A., 2012. Genesis of the glaciotectonic thrust-fault complex at Halk Hoved, southern Denmark. Bull. Geol. Soc. Den. 60, 61–80.
McBride, J.H., Pugin, A.J.M., Hatcher, R.D., 2007. Scale independence of décollement thrusting. In: Hatcher Jr., R.D., Carlson, M.P., McBride, J.H., Martínez Catalán, J.R. (Eds.), 4-D Framework of Continental Crust. Geol. Soc. Amer. Mem, vol. 200, pp. 109–126.
McClay, K.R., 1992. Glossary of thrust tectonic terms. In: McClay, K.R. (Ed.), Thrust Tectonics. Chapman & Hall, London, pp. 419–433.
Mellett, C.L., Phillips, E., Lee, J.R., Cotterill, C.J., Tjelta, T.I., James, L., Duffy, C., 2019. Elsterian ice-sheet retreat in the southern North Sea: antecedent controls on large-scale glaciotectonics and subglacial bed conditions. Boreas. https://doi.org/10.1111/bor.12410.
Meissner, R., Stegena, L., 1977. Praxis der seismischen Feldmessung und Auswertung. Gebrüder Bornträger, Berlin.
Meyer, K.-D., 1987. Ground and end moraines in lower Saxony. In: van der Meer, J.J.M. (Ed.), Tills and Glaciotectonics. Balkema, Rotterdam, pp. 197–204.
Meyer, K.-D., 1991. Zur Entstehung der westlichen der Ostsee. N. Jb. A 127, 429–446.
Miller, G.H., Mangerud, J., 1996. Aminostratigraphy of European marine interglacial deposits. Quat. Sci. Rev. 4, 215–278.
Moreau, J., Huuse, M., Janszen, A., Van der Vegt, P., Gibbard, P.L., Moscariello, A., 2012. The glaciogenic unconformity of the southern North Sea. In: Huuse, M., Redfern, J., Le Heron, D.P., Dixon, R.J., Moscariello, A., Craig, J. (Eds.), Glaciogenic Reservoirs, vol. 368. Geol. Soc. Spec. Pub., pp. 99–110
Moreau, J., Huuse, M., 2014. Infill of tunnel valleys associated with landward-flowing ice sheets: the missing Middle Pleistocene record of the NW European rivers? Geochem. Geophys. Geosyst. 15, 1–9.
Neben, S., (party chief) with contributions by the shipboard scientific party, 2004. Fahrtbericht/Cruise Report MV Aurelia Cruise BGR04-AUR–Nordsee–30.05.2004–19.06.2004. Unpublished. Bundesanstalt für Geowissenschaften und Rohstoffe, Hannover.
Neben, S., (party chief) with contributions by the shipboard scientific party, 2006. Fahrtbericht/Cruise Report RV Heincke Cruise HE242 Leg1–Nordsee 05–17.10.2005–14.11.2005. Unpublished. Bundesanstalt für Geowissenschaften und Rohstoffe, Hannover.
Nielsen, S.B., Gallagher, K., Leighton, C., Balling, N., Svenningsen, L., Jacobsen, B.H., Thomsen, E., Nielsen, O.B., Heilmann-Clausen, C., Egholm, M.A., Summerfield, M.A., Clausen, O.R., Piotrowski, J.A., Thorsen, M.R., Huuse, M.,

Abrahamsen, N., King, C., Lykke-Andersen, H., 2009. The evolution of western Scandinavian topography: a review of Neogene uplift versus the ICE (isostasy–climate–erosion) hypothesis. J. Geodyn. 47, 72–95.
Ó Cofaigh, C., Evans, D.J., Smith, I.R., 2010. Large-scale reorganization and sedimentation of terrestrial ice streams during late Wisconsinan Laurentide Ice Sheet deglaciation. Bull. Geol. Soc. Am. 122, 743–756.
Ottesen, D., Batchelor, C.L., Dowdeswell, J.A., Løseth, H., 2018. Morphology and pattern of quaternary sedimentation in the north Sea basin (52–62° N). Mar. Pet. Geol. 98, 836–859.
Overeem, I., Weltje, G.J., Bishop-Kay, C., Kroonenberg, S.B., 2001. The late Cenozoic Eridanos Delta system in the southern North Sea basin: a climate signal in sediment supply? Basin Res. 13, 293–312.
Panin, A., Astakhov, V., Komatsu, G., Lotsari, E., Lang, J., Winsemann, J., submitted for publication. Middle and Late Quaternary glacial lake-outburst floods, drainage diversions and reorganization of fluvial systems in northwestern Eurasia. Earth Sci. Rev.
Passchier, S., Laban, C., Mesdag, C.S., Rijsdijk, K.F., 2010. Subglacial bed conditions during Late Pleistocene glaciations and their impact on ice dynamics in the southern North Sea. Boreas 39, 633–647.
Pedersen, S.A.S., 1987. Comparative studies of gravity tectonics in Quaternary sediments and sedimentary rocks related to fold belts. In: Jones, M.E., Preston, R.M.F. (Eds.), Deformation of Sediments and Sedimentary Rocks, vol. 29. Geol. Soc. Lond. Spec. Publ., pp. 165–180
Pedersen, S.A.S., 1996. Progressive glaciotectonic deformation in Weichselian and Palaeogene deposits at Feggeklit, northern Denmark. Bull. Geol. Soc. Den. 42, 153–174.
Pedersen, S.A.S., 2005. Structural analysis of the Rubjerg Knude glaciotectonic complex, Vendsyssel, northern Denmark. Bull. Geol. Surv. Den. Green 8, 1–192.
Pedersen, S., 2014. Architecture of glaciotectonic complexes. Geoscience 4, 269–296.
Pedersen, S.A.S., Boldreel, L.O., 2017. Glaciotectonic deformations in the Jammerbugt and glaciodynamic development in the eastern North Sea. J. Quat. Sci. 32, 183–195.
Phillips, E.R., Evans, D.J.A., Auton, C.A., 2002. Polyphase deformation at an oscillating ice margin following the Loch Lomomd Readvance, central Scotland, UK. Sediment. Geol. 149, 157–182.
Phillips, E., Lee, J.R., Burke, H., 2008. Progressive proglacial to subglacial deformation and syntectonic sedimentation at the margins of the Mid-Pleistocene British Ice Sheet: evidence from north Norfolk, UK. Quat. Sci. Rev. 27, 1848–1871.
Phillips, E., Hodgson, D.M., Emery, A.R., 2017. The quaternary geology of the north Sea Basin. J. Quat. Sci. 32, 117–339.
Phillips, E., Cotterill, C., Johnson, K., Crombie, K., James, L., Carr, S., Ruiter, A., 2018. Large-scale glacitectonic deformation in response to active ice sheet retreat across Dogger Bank (southern central North Sea) during the Last Glacial Maximum. Quat. Sci. Rev. 179, 24–47.
Piotrowski, J.A., Larsen, N.K., Junge, F.W., 2004. Reflections on soft subglacial beds as a mosaic of deforming and stable spots. Quat. Sci. Rev. 23, 993–1000.
Prins, L.T., Andresen, K.J., 2019. Buried late Quaternary channel systems in the Danish North Sea–Genesis and geological evolution. Quat. Sci. Rev. 223, 105943.
Rasmussen, E.S., 2009. Neogene inversion of the central Graben and Ringkøbing-Fyn high, Denmark. Tectonophys 465, 84–97.
Rasmussen, E.S., Dybkjær, K., Piasecki, S., 2010. Lithostratigraphy of the upper Oligocene–Miocene succession of Denmark. Bull. Geol. Surv. Den. Greenl. 22, 1–92.
Rea, B.R., Newton, A.M., Lamb, R.M., Harding, R., Bigg, G.R., Rose, P., Spagnolo, M., Huuse, M., Cater, J.M.L., Archer, S., Buckley, F., Halliyeva, M., Huuse, J., Corrnwell, D.G., Brokelhurst, S.H., Howell, J.A., 2018. Extensive marine-terminating ice sheets in Europe from 2.5 million years ago. Sci. Adv. 4 (6), eaar8327.
Roberts, D.H., Evans, D.J., Callard, S.L., Clark, C.D., Bateman, M.D., Medialdea, A., Dove, D., Cotterill, C.J., Saher, M., Ó Cofaigh, C., Chiverrell, R.C., Moreton, S.G., Fabel, D., Bradwell, T., 2018. Ice marginal dynamics of the last British-Irish ice sheet in the southern North sea: ice limits, timing and the influence of the Dogger bank. Quat. Sci. Rev. 198, 181–207.
Roskosch, J., Winsemann, J., Polom, U., Brandes, C., Tsukamoto, S., Weitkamp, A., Bartholomäus, W.A., Henningsen, D., Frechen, M., 2015. Luminescence dating of ice-marginal deposits in northern Germany: evidence for repeated glaciations during the Middle Pleistocene (MIS 12 to MIS 6). Boreas 44, 103–126.
Rutten, M.G., 1960. Ice-pushed ridges, permafrost and drainage. Am. J. Sci. 258, 293–297.
Sandsersen, P.B.E., Jørgensen, F., 2017. Buried tunnel valleys in Denmark and their impact on the geological architecture of the sibsurface. Bull. Geol. Surv. Den. Greenl. 38, 13–16.
Sejrup, H.P., Hjelstuen, B.O., Dahlgren, K.T., Haflidason, H., Kuijpers, A., Nygård, A., Praeg, D., Stoker, M.S., Vorren, T.O., 2005. Pleistocene glacial history of the NW European continental margin. Mar. Pet. Geol. 22, 1111–1129.
Skupin, K., Zandstra, J.G., 2010. Gletscher der Saale-Kaltzeit am Niederrhein. Geologischer Dienst NRW, Krefeld.
Stackebrandt, W., 2009. Subglacial channels of Northern Germany – a brief review. Z. Deut. Ges. Geow 160, 203–210.
Stephan, H.-J., 2014. Climato-stratigraphic subdivision of the Pleistocene in Schleswig-Holstein, Germany and adjoining areas. E G Quat. Sci. J. 63, 3–18.
Stephan, H.-J., 2019. Fließrichtungen eiszeitlicher Gletscher in Schleswig-Holstein. Schrift. Naturwiss. Ver. Schleswig-Holstein 75 (in press).
Steinmetz, D., Winsemann, J., Brandes, C., Siemon, B., Ullmann, A., Wiederhold, H., Meyer, U., 2015. Towards an improved geological interpretation of airborne electromagnetic data: a case study from the Cuxhaven tunnel valley and its Neogene host sediments (northwest Germany). Neth. J. Geosci. 94, 201–227.
Stewart, M.A., 2016. Assemblage of buried and seabed tunnel valleys in the central North Sea: from morphology to ice-sheet dynamics. Geol. Soc. Lond. Mem. 46, 317–320.
Stewart, M.A., Lonergan, L., 2011. Seven glacial cycles in the middle-late Pleistocene of northwest Europe: geomorphic evidence from buried tunnel valleys. Geology 39, 283–286.
Stewart, M.A., Lonergan, L., Hampson, G., 2013. 3D seismic analysis of buried tunnel valleys in the central North Sea: morphology, cross-cutting generations and glacial history. Quat. Sci. Rev. 72, 1–17.
Stokes, C., Clark, C.D., 2001. Palaeo-ice streams. Quat. Sci. Rev. 20, 1437–1457.
Strayer, L.M., Hudleston, P.J., Lorig, L.J., 2001. A numerical model of deformation and fluid-flow in an evolving thrust wedge. Tectonophys 335, 121–145.
Streif, H., 2004. Sedimentary record of Pleistocene and Holocene marine inundations along the north sea coast of lower Saxony, Germany. Quat. Intern. 112, 3–28.
Szuman, I., Ewertowski, M., Kasprzak, L., 2013. Thermo-mechanical facies representative of fast and slow flowing ice sheets: the Weichselian ice sheet, a central west Poland case study. Proc. Geol. Assoc. 124, 818–833.
Tanner, D.C., Brandes, C., Leiss, B., 2010. Structure and kinematics of an outcrop-scale, fold-cored triangle zone. Bull. Am. Assoc. Pet. Geol. 94, 1799–1809.
Thöle, H., Gaedicke, C., Kuhlmann, G., Reinhardt, L., 2014. Late Cenozoic sedimentary evolution of the German North Sea–A seismic stratigraphic approach. Newsl. Stratigr. 47, 299–329.
Thomas, G.S.P., Chiverrell, R.C., 2007. Structural and depositional evidence for repeated ice-marginal oscillation along the eastern margin of the Late Devensian Irish Sea Ice Stream. Quat. Sci. Rev. 26, 2375–2405.
Toucanne, S., Zaragosi, S., Bourillet, J.F., Gibbard, P.L., Eynaud, F., Giraudeau, J., Turon, T.L., Cremer, M., Cortijo, E., Martinez, P., Rossignol, L., 2009. A 1.2 Ma record of glaciation and fluvial discharge for the west European Atlantic margin. Quat. Sci. Rev. 28, 2974–2981.
Tsui, P.C., Cruden, D.M., Thomson, S., 1989. Ice-thrust terrains and glaciotectonic settings in central Alberta. Can. J. Earth Sci. 26, 1308–1318.
Van der Wateren, D.F.M., 1985. A model of glacial tectonics, applied to the ice-pushed ridges in the Central Netherlands. Bull. Geol. Soc. Den. 34, 55–74.
Van der Wateren, F.M., 1995. Structural geology and sedimentology of push moraines. Med. Rijks Geol. Dienst Nr 54 (Haarlem).
Van Gijssel, K., 1987. A lithostratigraphic and glaciotectonic reconstruction of the Lamstedt moraine, lower Saxony (FRG). In: van der Meer, J.J.M. (Ed.), Tills and Glaciotectonics. Balkema, Rotterdam, pp. 145–155.
Vaughan-Hirsch, D.P., Phillips, E.R., 2017. Mid-pleistocene thin-skinned glaciotectonic thrusting of the Aberdeen Ground formation, central Graben region, Central North sea. J. Quat. Sci. 32, 196–212.
Vinx, R., Grube, A.T., Grube, F., 1997. Lithologie, Geschiebeführungund Geochemie eines Prä-Elster I-Tills von Lieth bei Elmshorn. Leipz. Geowiss. 5, 83–103.
Waller, R., Murton, J., Whiteman, C., 2009. Geological evidence for subglacial deformation of Pleistocene permafrost. Proc. Geol. Assoc. 120, 155–162.
Waller, R.I., Murton, J.B., Kristensen, L., 2012. Glacier–permafrost interactions: processes, products and glaciological implications. Sediment. Geol. 255, 1–28.
Włodarski, W., 2014. Geometry and kinematics of glaciotectonic deformation superimposed on the Cenozoic fault-tectonic framework in the central Polish Lowlands. Quat. Sci. Rev. 94, 44–61.
Winsemann, J., Lang, J., Roskosch, J., Polom, U., Böhner, U., Brandes, C., Glotzbach, C., Frechen, M., 2015. Terrace styles and timing of terrace formation in the Weser and Leine valleys, northern Germany: response of a fluvial system to climate change and glaciation. Quat. Sci. Rev. 123, 31–57.
Wunderlich, J., Müller, S., 2003. High-resolution sub-bottom profiling using parametric acoustics. Int. Ocean Syst. 7, 6–11.
Ziegler, P.A., 1990. Geological Atlas of Western and Central Europe. Shell Internationale Petroleum Maatshappij BV, The Hague.
Ziesch, J., Tanner, D.C., Krawczyk, C.M., 2014. Strain associated with the fault-parallel flow algorithm during kinematic fault displacement. Math. Geosci. 46, 59–73.